

# Reconstruction techniques for inverse Sturm-Liouville problems with complex coefficients

Vladislav V. Kravchenko

Departamento de Matemáticas, Cinvestav, Unidad Querétaro,  
 Libramiento Norponiente #2000, Fracc. Real de Juriquilla, Querétaro, Qro., 76230 MEXICO.  
 e-mail: vkravchenko@math.cinvestav.edu.mx

June 3, 2025

## Abstract

A variety of inverse Sturm-Liouville problems is considered, including the two-spectrum inverse problem, the problem of recovering the potential from the Weyl function, as well as the recovery from the spectral function. In all cases the potential in the Sturm-Liouville equation is assumed to be complex valued. A unified approach for the approximate solution of the inverse Sturm-Liouville problems is developed, based on Neumann series of Bessel functions (NSBF) representations for solutions and their derivatives. Unlike most existing approaches, it allows one to recover not only the complex-valued potential but also the boundary conditions of the Sturm-Liouville problem. Efficient accuracy control is implemented. The numerical method is direct. It involves only solving linear systems of algebraic equations for the coefficients of the NSBF representations, while eventually the knowledge only of the first NSBF coefficients leads to the recovery of the Sturm-Liouville problem. Numerical efficiency is illustrated by several test examples.

## 1 Introduction

Let  $q \in \mathcal{L}^2(0, b)$  be a complex-valued function. Consider the Sturm-Liouville equation

$$-y'' + q(x)y = \lambda y, \quad (1.1)$$

on a finite interval  $0 < x < b$ .

In the present work, we discuss a method for approximately solving a range of inverse spectral problems associated with equation (1.1). In particular, (i) the two-spectrum inverse problem; (ii) the recovery of the Sturm-Liouville problem from its Weyl function; (iii) the recovery of the Sturm-Liouville problem from a spectrum and corresponding multiplier constants, which represent the values of normalized eigenfunctions at endpoints; (iv) the recovery of the Sturm-Liouville problem from a spectrum and corresponding norming constants (weight numbers). While the method can be extended to more general situations, for simplicity, throughout this paper, we assume that the spectra considered are simple.

Development of efficient methods for solving inverse Sturm-Liouville problems is an active research area. Several methods have been proposed for the solution of inverse Sturm-Liouville problems of different types, which do not involve the techniques presented below (see [2], [7], [6], [9], [14], [17], [18], [20], [21], [38], [39], [40], [44], [45], [46] and many other publications). However, usually they require the knowledge of additional parameters like, e.g., the parameter  $\omega := \frac{1}{2} \int_0^b q(t) dt$  (such is the case of [20], [45], [46]) and do not allow the recovery of the boundary conditions. As an illustration of this

fact we quote [45, p. 177]: ‘as was mentioned earlier, if complete spectral data is available, then it is in theory possible to determine the boundary conditions as part of the solution of the problem. We do not believe, however, that this is numerically feasible in most cases.’ For this reason the boundary conditions are supposed to be known in all the above mentioned publications. Our approach is free of these restrictions, and moreover, to the difference from those previous publications, it allows us to recover complex valued potentials and complex constants from boundary conditions.

The overall approach presented here is based on Neumann series of Bessel functions (NSBF) representations for solutions of (1.1) and for their derivatives. The NSBF representations were derived in [31], where results on their convergence and on the decay rate for their coefficients can be found. In several publications, these NSBF representations have been applied successfully to solving inverse spectral problems. First, in [25], the classical problem of recovering the Sturm-Liouville problem from its spectral function (see problem (IP4) below) was approached with the aid of the NSBF and the Gelfand-Levitan integral equation. Due to the discontinuity of the sum of the series representing the Gelfand-Levitan integral kernel, the method provided less accuracy near endpoints. In [26, Sect. 13.4] its simple modification was proposed, solving this particular problem. In [24] another series representation for the Gelfand-Levitan kernel was derived, such that the sum of the series became continuous. This was used in [33] to improve the approach from [25]. The approach based on using the NSBF combined with the Gelfand-Levitan integral equation was applied to other inverse Sturm-Liouville problems, both on a finite interval and on a half-line [13], [23], [22], [26, Sect. 13.4], [32], [33], [34], [35].

Another way of applying NSBF representations to coefficient inverse problems was explored in [29], [27], [5], [3], [4], [12]. From the input data of the problem and by computing NSBF coefficients (evaluated at  $x = b$ ), a couple of the characteristic functions of certain Sturm-Liouville problems were computed. They were used for computing a spectrum and a sequence of corresponding multiplier constants (which relate the linearly dependent eigenfunctions normalized at opposite endpoints), thus reducing the original problem to problem (IP3) below, which was solved by substituting NSBF into the relation between the linearly dependent eigenfunctions and solving the resulting system of linear algebraic equations. This scheme works well. The spectrum and the multiplier constants are computed in great quantities and with a remarkable and uniform accuracy. It is also interesting to note that this approach allows one to compute spectra of Sturm-Liouville problems from other input data and without knowing the potential  $q(x)$ . Moreover, one even can complete a spectrum, i.e., by given several first eigenvalues of a Sturm-Liouville problem to compute much more of them, again without knowing  $q(x)$  [27]. Nevertheless, this approach is restricted to real valued potentials, since computing complex eigenvalues is a challenging task.

Another approach, which does not require computing eigenvalues, and therefore, it is suitable for complex-valued potentials, was proposed in [28] for solving a coefficient inverse problem for (1.1). For obtaining the main system of linear algebraic equations for the NSBF coefficients, instead of the relation between the linearly dependent eigenfunctions another identity, relating three different solutions of (1.1) was used (see identity (3.3) below). In the present work we develop further this idea and devise an approach, which allows one to solve a wide variety of inverse Sturm-Liouville problems for equation (1.1) with a complex-valued potential  $q(x)$ , including the recovery of the unknown constants in the boundary conditions. It is based on the NSBF representations and several identities for solutions of (1.1). The overall scheme reduces the solution of an inverse problem to solving a couple of systems of linear algebraic equations. The potential and constants are recovered from the very first NSBF coefficients. The resulting numerical method is simple, accurate and fast. Several practical criteria are derived for choosing the involved parameters and ensuring accuracy. The method requires neither additional assumptions on the potential nor initial guesses and does not involve any iterative procedures. Thus, the contribution of this work consists of a universal approach to the approximate

solution of a wide range of inverse Sturm-Liouville problems for equation (1.1).

## 2 Two-spectrum inverse problem setting

Let  $q \in \mathcal{L}^2(0, b)$  be complex valued,  $b > 0$ . Consider the Sturm-Liouville equation

$$-y'' + q(x)y = \lambda y, \quad x \in (0, b), \quad (2.1)$$

where  $\lambda \in \mathbb{C}$  is a spectral parameter.

Denote by  $L = L(q(x), h, H)$  the Sturm-Liouville problem for (2.1) with the boundary conditions

$$U(y) := y'(0) - hy(0) = 0, \quad V(y) := y'(b) + Hy(b) = 0, \quad (2.2)$$

where  $h$  and  $H$  are some complex constants.

Denote by  $L^0 = L^0(q(x), H)$  the Sturm-Liouville problem for (2.1) with the boundary conditions

$$y(0) = 0, \quad V(y) = 0. \quad (2.3)$$

Theory of problems  $L$  and  $L^0$  is well developed (see, [41], [8], [10]). In particular, the spectrum of each problem is discrete, and a finite number of the eigenvalues can have multiplicities greater than one. However, for simplicity, throughout this paper we assume that the spectra considered are simple.

We start by considering the classical two-spectrum inverse problem, which is formulated as follows (the other inverse Sturm-Liouville problems considered in the present work, are introduced in Section 5).

**Inverse Problem (IP1)** Given two spectra  $\{\lambda_k\}_{k=0}^\infty$  and  $\{\lambda_k^0\}_{k=0}^\infty$  of problems  $L$  and  $L^0$ , respectively, find  $q(x) \in \mathcal{L}^2(0, b)$  and the constants  $h, H$ .

For the uniqueness result for (IP1) we refer to [8], [10], and for the stability result for (IP1) to [11].

The primary result of this study is a method for approximating the solution of (IP1) when a finite number of eigenpairs  $\{\lambda_k, \lambda_k^0\}_{k=0}^K$  are available. Often it is convenient to deal with the square root of the spectral parameter:  $\rho = \sqrt{\lambda}$ . Since it is not essential which of the square roots is chosen, we can always assume that  $\text{Im } \rho \geq 0$ . Denote  $\rho_k = \sqrt{\lambda_k}$  and  $\mu_k = \sqrt{\lambda_k^0}$  the square roots of the eigenvalues of problems  $L$  and  $L^0$ , respectively. Sometimes  $\rho_k$  and  $\mu_k$  are called singular numbers of the respective Sturm-Liouville problems.

## 3 Solutions and their series representations

Let  $\varphi_h(\rho, x)$ ,  $S(\rho, x)$ ,  $\psi_H(\rho, x)$ ,  $T(\rho, x)$  denote the solutions of (2.1) satisfying the respective initial conditions

$$\begin{aligned} \varphi_h(\rho, 0) &= 1, & \varphi_h'(\rho, 0) &= h, & S(\rho, 0) &= 0, & S'(\rho, 0) &= 1, \\ \psi_H(\rho, b) &= 1, & \psi_H'(\rho, b) &= -H, & T(\rho, b) &= 0, & T'(\rho, b) &= 1. \end{aligned}$$

For all  $\rho \in \mathbb{C}$ , we have  $U(\varphi_h) = 0$  and  $V(\psi_H) = 0$ . Denote

$$\Delta(\rho) = W[\psi_H(\rho, x), \varphi_h(\rho, x)],$$

where  $W$  stands for the Wronskian (we recall that the Wronskian of any pair of solutions of (2.1) is independent of  $x$ ). Substituting  $x = 0$  and  $x = b$ , we find out that

$$\Delta(\rho) = V(\varphi_h) = -U(\psi_H). \quad (3.1)$$

The set of zeros of  $\Delta(\rho)$  coincides with the set of the singular numbers  $\rho_k$  of problem  $L$ . Thus,  $\Delta(\rho)$  is a characteristic function of problem  $L$ . Analogously, the characteristic function of problem  $L^0$  has the form

$$\Delta^0(\rho) = \psi_H(\rho, 0) = S'(\rho, b) + HS(\rho, b).$$

The following easily verifiable identities hold

$$\psi_H(\rho, x) = \Delta^0(\rho) \varphi_h(\rho, x) - \Delta(\rho) S(\rho, x) \quad (3.2)$$

and

$$T(\rho, x) = \varphi_h(\rho, b) S(\rho, x) - S(\rho, b) \varphi_h(\rho, x). \quad (3.3)$$

We will use the following series representations for the solutions, derived in [31].

**Theorem 3.1 ([31])** *The solutions  $\varphi_h(\rho, x)$ ,  $S(\rho, x)$ ,  $\psi_H(\rho, x)$ ,  $T(\rho, x)$  admit the following series representations*

$$\varphi_h(\rho, x) = \cos \rho x + \sum_{n=0}^{\infty} (-1)^n g_n(x) \mathbf{j}_{2n}(\rho x), \quad (3.4)$$

$$S(\rho, x) = \frac{\sin \rho x}{\rho} + \frac{1}{\rho} \sum_{n=0}^{\infty} (-1)^n s_n(x) \mathbf{j}_{2n+1}(\rho x), \quad (3.5)$$

$$\psi_H(\rho, x) = \cos(\rho(x-b)) + \sum_{n=0}^{\infty} (-1)^n \psi_n(x) \mathbf{j}_{2n}(\rho(x-b)), \quad (3.6)$$

$$T(\rho, x) = \frac{\sin(\rho(x-b))}{\rho} + \frac{1}{\rho} \sum_{n=0}^{\infty} (-1)^n t_n(x) \mathbf{j}_{2n+1}(\rho(x-b)). \quad (3.7)$$

where  $\mathbf{j}_k(z)$  stands for the spherical Bessel function of order  $k$  ( $\mathbf{j}_k(z) := \sqrt{\frac{\pi}{2z}} J_{k+\frac{1}{2}}(z)$ , see, e.g., [1]). For every  $\rho \in \mathbb{C}$  the series converge pointwise. For every  $x \in [0, L]$  the series converge uniformly in any strip of the complex plane of the variable  $\rho$ , parallel to the real axis. In particular, the remainders of their partial sums  $\varphi_{h,N}(\rho, x) := \cos \rho x + \sum_{n=0}^N (-1)^n g_n(x) \mathbf{j}_{2n}(\rho x)$  and  $S_N(\rho, x) := \frac{\sin \rho x}{\rho} + \frac{1}{\rho} \sum_{n=0}^N (-1)^n s_n(x) \mathbf{j}_{2n+1}(\rho x)$  admit the estimates

$$|\varphi(\rho, x) - \varphi_{h,N}(\rho, x)| \leq \frac{\varepsilon_N(x) \sinh(ax)}{a} \quad \text{and} \quad |\rho S(\rho, x) - \rho S_N(\rho, x)| \leq \frac{\varepsilon_N(x) \sinh(ax)}{a} \quad (3.8)$$

for any  $\rho$  belonging to a strip  $|\operatorname{Im} \rho| \leq a$ ,  $a > 0$ , where  $\varepsilon_N(x)$  is a positive function tending to zero when  $N \rightarrow \infty$ . Analogous estimates are valid for the remainders of the series (3.6) and (3.7).

The first coefficients of the series have the form

$$g_0(x) = \varphi_h(0, x) - 1, \quad s_0(x) = 3 \left( \frac{S(0, x)}{x} - 1 \right), \quad (3.9)$$

$$\psi_0(x) = \psi_H(0, x) - 1, \quad t_0(x) = 3 \left( \frac{T(0, x)}{x-b} - 1 \right), \quad (3.10)$$

and the rest of the coefficients can be calculated following a simple recurrent integration procedure.

Analogous series representations are also available for the derivatives of the solutions [31]. In particular, we will use the series representations

$$\varphi'_h(\rho, x) = -\rho \sin(\rho x) + (h + \omega(x)) \cos(\rho x) + \sum_{n=0}^{\infty} (-1)^n \gamma_n(x) \mathbf{j}_{2n}(\rho x), \quad (3.11)$$

and

$$S'(\rho, x) = \cos(\rho x) + \frac{\omega(x)}{\rho} \sin(\rho x) + \frac{1}{\rho} \sum_{n=0}^{\infty} (-1)^n \sigma_n(x) \mathbf{j}_{2n+1}(\rho x), \quad (3.12)$$

where

$$\omega(x) := \frac{1}{2} \int_0^x q(t) dt,$$

and the first coefficients have the form

$$\gamma_0(x) = g'_0(x) - \omega(x), \quad \sigma_0(x) = \frac{s_0(x)}{x} + s'_0(x) - 3\omega(x).$$

Again, the rest of the coefficients can be calculated following a simple recurrent integration procedure, and the series (3.11) and (3.12) converge uniformly in any strip of the complex plane of the variable  $\rho$ , parallel to the real axis.

We recall that according to [48, p. 522]: ‘Any series of the type

$$\sum_{n=0}^{\infty} a_n J_{\nu+n}(z) \quad (3.13)$$

is called a Neumann series, although in fact Neumann considered only the special type of series for which  $\nu$  is an integer; the investigation of the more general series is due to Gegenbauer.’ Since in functional analysis, the term Neumann series is often used for referring to series of another nature, the series (3.13) are often referred to as Neumann series of Bessel functions (NSBF) (see, e.g., [49]). Thus, we will refer to the series representations for the solutions and their derivatives, which are used in the present work, as NSBF representations.

**Remark 3.2** *The NSBF representations are the result of the series expansions of the transformation (transmutation) operator kernels into corresponding series in terms of Legendre polynomials. Namely, as it is well known (see, e.g., [15], [37], [41], [47]) there exist continuous functions  $\mathbf{G}_h(x, t)$  and  $\mathbf{S}(x, t)$  in the domain  $0 \leq t \leq x \leq b$ , such that*

$$\varphi_h(\rho, x) = \cos \rho x + \int_0^x \mathbf{G}_h(x, t) \cos \rho t dt,$$

$$S(\rho, x) = \frac{\sin \rho x}{\rho} + \int_0^x \mathbf{S}(x, t) \frac{\sin \rho t}{\rho} dt$$

for all  $\rho \in \mathbb{C}$ . These Volterra integral operators of the second kind are known as the transformation operators. Among the properties of the kernels  $\mathbf{G}_h(x, t)$  and  $\mathbf{S}(x, t)$  we will use the equalities

$$\mathbf{G}_h(x, x) = h + \omega(x), \quad \mathbf{S}(x, x) = \omega(x). \quad (3.14)$$

In [31] the following series expansions for  $\mathbf{G}_h(x, t)$  and  $\mathbf{S}(x, t)$  were obtained

$$\mathbf{G}_h(x, t) = \sum_{n=0}^{\infty} \frac{g_n(x)}{x} P_{2n} \left( \frac{t}{x} \right), \quad \mathbf{S}(x, t) = \sum_{n=0}^{\infty} \frac{s_n(x)}{x} P_{2n+1} \left( \frac{t}{x} \right),$$

where  $P_k$  stands for the Legendre polynomial of degree  $k$ , and the coefficients  $g_n(x)$  and  $s_n(x)$  are those from Theorem 3.1. Since  $P_k(1) = 1$  for all  $k \in \mathbb{N} \cup \{0\}$ , we have

$$\sum_{n=0}^{\infty} \frac{g_n(x)}{x} = h + \omega(x), \quad \sum_{n=0}^{\infty} \frac{s_n(x)}{x} = \omega(x).$$

Thus,

$$\frac{1}{x} \sum_{n=0}^{\infty} (g_n(x) - s_n(x)) = h. \quad (3.15)$$

**Remark 3.3** Since  $\varphi_h(0, x) = g_0(x) + 1$ , we have that

$$q(x) = \frac{\varphi_h''(0, x)}{\varphi_h(0, x)} = \frac{g_0''(x)}{g_0(x) + 1}.$$

That is,  $q(x)$  can be recovered directly from the first coefficient  $g_0(x)$ , or, analogously, from  $\psi_0(x)$ :

$$q(x) = \frac{\psi_0''(x)}{\psi_0(x) + 1},$$

or from a linear combination of  $g_0(x)$  and  $\psi_0(x)$ . Moreover, we have

$$g'_0(0) = \varphi'_h(0, 0) = h \quad \text{and} \quad \psi'_0(b) = \psi'_H(0, b) = -H,$$

and hence the constants  $h$  and  $H$  can also be recovered from the first NSBF coefficients  $g_0(x)$  and  $\psi_0(x)$ .

## 4 Approximate solution of inverse problem (IP1)

The overall approach to solving the inverse problem (IP1) involves working with the NSBF coefficients of the solutions and their derivatives. In the first step, we solve a system of linear algebraic equations to compute the characteristic functions  $\Delta(\rho)$  and  $\Delta^0(\rho)$ , while in the second, with their aid we construct another system of linear algebraic equations for the NSBF coefficients of the solutions  $\varphi_h(\rho, x)$ ,  $S(\rho, x)$  and  $\psi_H(\rho, x)$ . For this, identity (3.2) is used. Finally the potential  $q(x)$  and the constants  $h$ ,  $H$  are computed from the first NSBF coefficients  $g_0(x)$  and  $\psi_0(x)$  as explained in Remark 3.3.

### 4.1 Reconstruction of characteristic functions $\Delta(\rho)$ and $\Delta^0(\rho)$

#### 4.1.1 Recovering $\Delta^0(\rho)$

For any singular number  $\mu_k$  of problem  $L^0$  we have the equality  $\psi_H(\mu_k, 0) = 0$ , which can be written in the form

$$\sum_{n=0}^{\infty} (-1)^n \psi_n(0) \mathbf{j}_{2n}(\mu_k b) = -\cos(\mu_k b).$$

Let us assume that a number of the eigenpairs  $\rho_k = \sqrt{\lambda_k}$  and  $\mu_k = \sqrt{\lambda_k^0}$  are given for  $k = 0, \dots, K$ . Considering a partial sum of the series and writing down a corresponding equation for each known  $\mu_k$ , we obtain the system of linear algebraic equations for the coefficients  $\psi_n(0)$ :

$$\sum_{n=0}^{N_1} (-1)^n \psi_n(0) \mathbf{j}_{2n}(\mu_k b) = -\cos(\mu_k b), \quad k = 0, \dots, K. \quad (4.1)$$

Here  $N_1$  needs to be less or equal  $K$ . Solving this system leads to an approximation of the characteristic function  $\Delta^0(\rho)$ , which we denote by  $\Delta_{N_1}^0(\rho)$ :

$$\Delta_{N_1}^0(\rho) = \cos(\rho b) + \sum_{n=0}^{N_1} (-1)^n \psi_n(0) \mathbf{j}_{2n}(\rho b).$$

It gives us an approximation of  $\Delta^0(\rho)$ . According to the estimates from Theorem 3.1, it is expected to provide more accurate results for  $\rho$  belonging to a strip  $|\operatorname{Im} \rho| \leq a$ , where  $a \geq 0$  should not be too large.

#### 4.1.2 Recovering $\Delta(\rho)$

Next, we consider the singular numbers  $\rho_k$ . We have the equality  $\Delta(\rho_k) = 0$ , which can be written as  $\varphi'_h(\rho_k, b) + H\varphi_h(\rho_k, b) = 0$  or, equivalently,

$$\omega_{h,H} \cos(\rho_k b) + \sum_{n=0}^{\infty} (-1)^n \gamma_n(b) \mathbf{j}_{2n}(\rho_k b) + H \sum_{n=0}^{\infty} (-1)^n g_n(b) \mathbf{j}_{2n}(\rho_k b) = \rho_k \sin(\rho_k b),$$

where  $\omega_{h,H} := h + H + \omega(b)$ . Denote

$$h_n := (-1)^n (\gamma_n(b) + H g_n(b)), \quad n = 0, 1, \dots$$

Then

$$\omega_{h,H} \cos(\rho_k b) + \sum_{n=0}^{\infty} h_n \mathbf{j}_{2n}(\rho_k b) = \rho_k \sin(\rho_k b).$$

Considering a partial sum of the series and writing down corresponding equations for all available values  $\rho_k$ , we obtain a system of linear algebraic equations for the unknowns  $\omega_{h,H}$  and  $\{h_n\}_{n=0}^{N_2}$  in the form

$$\omega_{h,H} \cos(\rho_k b) + \sum_{n=0}^{N_2} h_n \mathbf{j}_{2n}(\rho_k b) = \rho_k \sin(\rho_k b), \quad k = 0, \dots, K. \quad (4.2)$$

Here  $N_2 \leq K - 1$ . For simplicity, we will assume that  $N_2 = N_1$ , and hence this is a system of linear algebraic equations for  $N_1 + 2$  unknowns:  $\omega_{h,H}$ ,  $\{h_n\}_{n=0}^{N_1}$ . Solving (4.2) gives us an approximation of  $\Delta(\rho)$ :

$$\Delta_{N_2}(\rho) = \omega_{h,H} \cos(\rho b) - \rho \sin(\rho b) + \sum_{n=0}^{N_1} h_n \mathbf{j}_{2n}(\rho b).$$

#### 4.1.3 Choosing the number of the coefficients

For a detailed analysis of systems of the type (4.1) and (4.2) we refer to [33], where it was explained that making (4.1) and (4.2) square sometimes can lead to worse numerical results, because the systems may become ill-conditioned. However, no criterion was proposed for choosing an optimal value of  $N_1$ . Here we fill this gap by proposing such a simple and viable criterion. To this purpose, it is convenient to compute a number of the coefficients  $\{s_n(b), g_n(b)\}_{n=0}^{N_1}$ . For this, note that since  $\Delta^0(\mu_k) = 0$ , from (3.2) we have that  $\psi_H(\mu_k, x) = -\Delta(\mu_k) S(\mu_k, x)$ . Hence for  $x = b$ :

$$S(\mu_k, b) = -\frac{1}{\Delta(\mu_k)}. \quad (4.3)$$

The values of  $\Delta(\mu_k)$  are computed with the aid of the computed previously  $\omega_{h,H}$ ,  $\{h_n\}_{n=0}^{N_1}$ . We have  $\Delta(\mu_k) \cong \Delta_{N_1}(\mu_k) = \omega_{h,H} \cos(\mu_k b) - \mu_k \sin(\mu_k b) + \sum_{n=0}^{N_1} h_n \mathbf{j}_{2n}(\mu_k b)$ . Thus, for the coefficients  $\{s_n(b)\}_{n=0}^{N_1}$  we obtain the system

$$\sum_{n=0}^{N_1} (-1)^n s_n(b) \mathbf{j}_{2n+1}(\mu_k b) = -\left( \sin \mu_k b + \frac{\mu_k}{\Delta_{N_1}(\mu_k)} \right), \quad k = 0, \dots, K. \quad (4.4)$$

Analogously, observe that for  $\rho = \rho_k$  identity (3.2) gives  $\psi_H(\rho_k, x) = \Delta^0(\rho_k) \varphi_h(\rho_k, x)$ , which for  $x = b$  leads to the equality

$$\varphi_h(\rho_k, x) = \frac{1}{\Delta^0(\rho_k)}.$$

Thus, a number of the coefficients  $\{g_n(b)\}_{n=0}^{N_1}$  can be computed from the system

$$\sum_{n=0}^{N_1} (-1)^n g_n(b) \mathbf{j}_{2n}(\rho_k b) = \frac{1}{\Delta_{N_1}^0(\rho_k)} - \cos \rho_k b, \quad k = 0, \dots, K, \quad (4.5)$$

where the values of  $\Delta_{N_1}^0(\rho_k)$  are computed with the aid of the computed previously  $\{\psi_n(0)\}_{n=0}^{N_1}$ :  $\Delta_{N_1}^0(\rho_k) = \cos(\rho_k b) + \sum_{n=0}^{N_1} (-1)^n \psi_n(0) \mathbf{j}_{2n}(\rho_k b)$ .

Now, for a given  $K$ , a convenient choice of  $N_1$  can be made in two ways, both by using identity (3.2). For  $x = b$ , identity (3.2) turns into the equality

$$\Delta^0(\rho) \varphi_h(\rho, b) - \Delta(\rho) S(\rho, b) = 1.$$

Choosing a set of points  $\rho = r_j$ ,  $j = 1, \dots, J$ , where  $J$  can be arbitrarily large, and  $|\operatorname{Im} r_j| \leq a$  (with a reasonably large  $a$  or  $a = 0$ ), one can compute the functional

$$P(N_1) := \max_j \left| \Delta_{N_1}^0(r_j) \varphi_{h, N_1}(r_j, b) - \Delta_{N_1}(r_j) S_{N_1}(r_j, b) - 1 \right|,$$

which provides information on the accuracy attained for the chosen  $N_1$ . Minimization of  $P(N_1)$  gives us a suitable choice of  $N_1$ .

Another criterion for choosing  $N_1$  can be devised as follows. Consider identity (3.2) for  $x = b$  and  $\rho = 0$ :

$$1 = (1 + \psi_0(0)) (1 + g_0(b)) - b (\omega_{h, H} + h_0) \left( 1 + \frac{s_0(b)}{3} \right),$$

or equivalently,

$$g_0(b) (1 + \psi_0(0)) + \psi_0(0) - \frac{b}{3} (\omega_{h, H} + h_0) (3 + s_0(b)) = 0.$$

Define

$$R(N_1) := \left| g_0(b) (1 + \psi_0(0)) + \psi_0(0) - \frac{b}{3} (\omega_{h, H} + h_0) (3 + s_0(b)) \right|,$$

where all the magnitudes are computed with the parameter  $N_1$  in systems (4.1), (4.2), (4.4), (4.5). Minimizing  $R(N_1)$  gives us another criterion for the choice of a suitable value of  $N_1$ . Obviously, this criterion is especially useful when zero is not an eigenvalue neither of problem  $L$  nor of  $L^0$ .

It turns out that both criteria deliver similar results, as we show below. Thus, one can use the value  $N_1$  which minimizes  $R(N_1)$ , since the computation of  $R(N_1)$  is easier and faster.

## 4.2 Reconstruction of $q(x)$ , $h$ and $H$

In the second step we use identity (3.2), where  $\Delta^0(\rho)$  and  $\Delta(\rho)$  are already approximated by  $\Delta_{N_1}^0(\rho)$  and  $\Delta_{N_1}(\rho)$ , respectively, and the solutions  $\psi_H(\rho, x)$ ,  $\varphi_h(\rho, x)$  and  $S(\rho, x)$  are replaced by their NSBF representations. Thus, choosing a set of points  $\{r_j\}_{j=1}^J \subset \mathbb{R}$  sufficiently large, for any  $x \in (0, b)$  we consider the system of linear algebraic equations for the NSBF coefficients

$$\begin{aligned} \Delta_{N_1}^0(r_j) \sum_{n=0}^{N_3} (-1)^n g_n(x) \mathbf{j}_{2n}(r_j x) - \frac{\Delta(r_j)}{r_j} \sum_{n=0}^{N_3} (-1)^n s_n(x) \mathbf{j}_{2n+1}(r_j x) - \sum_{n=0}^{N_3} (-1)^n \psi_n(x) \mathbf{j}_{2n}(r_j(x-b)) \\ = \cos(r_j(x-b)) - \Delta_{N_1}^0(r_j) \cos(r_j x) + \frac{\Delta(r_j)}{r_j} \sin(r_j x), \quad j = 1, \dots, J, \end{aligned} \quad (4.6)$$

where  $3(N_3 + 1) \leq J$ . Solving this system for a sufficiently dense set of points  $x \in (0, b)$  gives us the values of  $g_0(x)$  and  $\psi_0(x)$ . Note that there is no need to solve system (4.6) at the endpoints, because the values of  $g_0(x)$  and  $\psi_0(x)$  there are already known. We have that  $g_0(0) = \psi_0(b) = 0$  (see (3.9) and (3.10)), while the values  $g_0(b)$  and  $\psi_0(0)$  were computed in the first step.

Finally,  $q(x)$ ,  $h$  and  $H$  are recovered from  $g_0(x)$  and  $\psi_0(x)$  as explained in Remark 3.3.

## 5 Approximate solution of other inverse spectral problems

In this section we show that the approach presented above is quite universal and can be easily adapted for solving a wide variety of inverse spectral problems. In particular, we consider the recovery from Weyl's function; from one spectrum and multiplier constants (which are values of normalized eigenfunctions at endpoints); from one spectrum and a sequence of norming constants.

### 5.1 Recovery from Weyl function

Let  $\Phi(\rho, x)$  be a solution of (2.1) satisfying the boundary conditions

$$U(\Phi) = 1, \quad V(\Phi) = 0.$$

The solution  $\Phi(\rho, x)$  is known as the Weyl solution. The Weyl function of problem  $L$  is then defined as

$$M(\rho) := \Phi(\rho, 0)$$

(see, e.g., [50, Sect. 1.2]).

Consider the following inverse problem.

**Inverse Problem (IP2)** Given the Weyl function  $M(\rho)$ , find  $q(x) \in \mathcal{L}^2(0, b)$  and the constants  $h$ ,  $H$ , such that  $M(\rho)$  be the Weyl function of problem  $L$ .

More precisely, we are interested in the approximate solution of (IP2) when  $M(\rho)$  is given on a finite set of points  $\{\rho = z_k\}_{k=1}^{K_1}$ .

It is easy to see that

$$\Phi(\rho, x) = S(\rho, x) + M(\rho)\varphi_h(\rho, x).$$

Hence

$$V(\Phi) = S'(\rho, b) + HS(\rho, b) + M(\rho)(\varphi'_h(\rho, b) + H\varphi_h(\rho, b)) = 0,$$

or equivalently,

$$\Delta^0(\rho) + M(\rho)\Delta(\rho) = 0. \tag{5.1}$$

Substitution of  $\rho = z_k$ ,  $k = 1, \dots, K_1$  and of the NSBF representations (truncated up to some  $N_1$ ) leads to the system of linear algebraic equations for the NSBF coefficients  $\omega_{h,H}$ ,  $\{\psi_n(0)\}$  and  $\{h_n\}$ :

$$\sum_{n=0}^{N_1} (-1)^n \psi_n(0) \mathbf{j}_{2n}(z_k b) + M(z_k) \omega_{h,H} \cos(z_k b) + M(z_k) \sum_{n=0}^{N_1} h_n \mathbf{j}_{2n}(z_k b) = M(z_k) z_k \sin(z_k b) - \cos(z_k b), \tag{5.2}$$

$k = 1, \dots, K_1$ ,  $2(N_1 + 1) \leq K_1 - 1$ . Solving this system gives us the approximations  $\Delta_{N_1}^0(\rho)$  and  $\Delta_{N_1}(\rho)$ , after which we proceed to the second step, see subsection 4.2.

## 5.2 Recovery from eigenvalues and multiplier constants

Let  $\rho_k$  be a singular value of problem  $L$ . We have that the solutions  $\varphi_h(\rho_k, x)$  and  $\psi_H(\rho_k, x)$  are necessarily linearly dependent, so there exists a constant  $\beta_k \neq 0$  such that

$$\varphi_h(\rho_k, x) = \beta_k \psi_H(\rho_k, x). \quad (5.3)$$

Choosing here  $x = 0$  and  $x = b$ , we obtain that

$$\beta_k = \frac{1}{\psi_H(\rho_k, 0)} = \varphi_h(\rho_k, b). \quad (5.4)$$

Now the following inverse problem is considered.

**Inverse Problem (IP3)** Given the singular values  $\{\rho_k\}_{k=0}^{\infty}$  and the multiplier constants  $\{\beta_k\}_{k=0}^{\infty}$  of problem  $L$ , find  $q(x) \in \mathcal{L}^2(0, b)$  and the constants  $h, H$ .

A similar inverse problem was considered in [9], however with boundary conditions not containing unknown constants and for real valued  $q(x)$ . We also note that it is often convenient to reduce other types of inverse spectral problems to (IP3) (see [3], [4], [12], [27]). Our approach allows us to solve this problem numerically in one step. Indeed, equality (5.3) leads to the following system of linear algebraic equations for the NSBF coefficients of the solutions  $\varphi_h(\rho, x)$  and  $\psi_H(\rho, x)$ :

$$\sum_{n=0}^{\infty} (-1)^n g_n(x) \mathbf{j}_{2n}(\rho_k x) - \beta_k \sum_{n=0}^{\infty} (-1)^n \psi_n(x) \mathbf{j}_{2n}(\rho_k (x - b)) = \beta_k \cos(\rho_k (x - b)) - \cos(\rho_k x), \quad (5.5)$$

$k = 0, 1, \dots$  Solving this system, or its truncated version approximately on a sufficiently dense set of points  $x \in [0, b]$ , we find  $g_0(x)$  and  $\psi_0(x)$  and apply Remark 3.3 for recovering  $q(x)$ ,  $h$  and  $H$ . Here unlike the solution of (4.6) in subsection 4.2, we solve (5.5) at the endpoints as well, where it is convenient to take into account that  $g_n(0) = \psi_n(b) = 0$ ,  $n = 0, 1, \dots$

This direct way to solve (IP3) in one step, possibly, is not the best option for numerical computations. It requires a relatively large number of the data to be given. Another possibility leads to overall better numerical results. First, by the given  $\rho_k$  we approximate  $\Delta(\rho)$ . This is done exactly as in subsection 4.1.2. Next, we use  $\beta_k$  for computing a number of the coefficients  $\psi_n(0)$ . Namely, we have  $\psi_H(\rho_k, 0) = 1/\beta_k$ ,  $k = 0, 1, \dots$ . This gives us the system of linear algebraic equations for the coefficients  $\psi_n(0)$ :

$$\sum_{n=0}^{N_1} (-1)^n \psi_n(0) \mathbf{j}_{2n}(\rho_k b) = \frac{1}{\beta_k} - \cos(\rho_k b), \quad k = 0, \dots, K$$

(compare to (4.1)).

Thus, again, we have approximated  $\Delta^0(\rho)$  and  $\Delta(\rho)$  by  $\Delta_{N_1}^0(\rho)$  and  $\Delta_{N_1}(\rho)$ , which leads us to the second step of the method, explained in subsection 4.2.

## 5.3 Recovery from eigenvalues and norming constants

For every singular value  $\rho_k$  of problem  $L$ , we denote by  $\alpha_k$  the corresponding norming constant

$$\alpha_k := \int_0^b \varphi_h^2(\rho_k, x) dx.$$

Consider the inverse problem.

**Inverse Problem (IP4)** Given the singular values  $\{\rho_k\}_{k=0}^{\infty}$  and the norming constants  $\{\alpha_k\}_{k=0}^{\infty}$  of problem  $L$ , find  $q(x) \in \mathcal{L}^2(0, b)$  and the constants  $h, H$ .

We recall that

$$\frac{\alpha_k}{\beta_k} = -\frac{\dot{\Delta}(\rho_k)}{2\rho_k}, \quad (5.6)$$

where  $\dot{\Delta}$  means the derivative with respect to  $\rho$ . Indeed, with the aid of the equality

$$\frac{d}{dx} W[\psi_H(\rho, x), \varphi_h(\rho_k, x)] = (\rho^2 - \rho_k^2) \psi_H(\rho, x) \varphi_h(\rho_k, x)$$

we obtain

$$(\rho^2 - \rho_k^2) \int_0^b \psi_H(\rho, x) \varphi_h(\rho_k, x) dx = W[\psi_H(\rho, x), \varphi_h(\rho_k, x)]|_0^b = -\Delta(\rho),$$

or

$$\frac{\Delta(\rho)}{(\lambda - \lambda_k)} = -\int_0^b \psi_H(\rho, x) \varphi_h(\rho_k, x) dx,$$

which at the limit  $\lambda \rightarrow \lambda_k$  gives us (5.6).

Thus,

$$\beta_k = -\frac{2\rho_k \alpha_k}{\dot{\Delta}(\rho_k)}. \quad (5.7)$$

It is easy to obtain an NSBF representation for  $\dot{\Delta}(\rho)$ . We have

$$\Delta(\rho) = \omega_{h,H} \cos(\rho b) - \rho \sin(\rho b) + \sum_{n=0}^{\infty} h_n \mathbf{j}_{2n}(\rho b).$$

Hence

$$\dot{\Delta}(\rho) = -(1 + b\omega_{h,H}) \sin(\rho b) - \rho b \cos(\rho b) + \sum_{n=0}^{\infty} h_n \left( b \mathbf{j}_{2n+1}(\rho b) - \frac{2n}{\rho} \mathbf{j}_{2n}(\rho b) \right). \quad (5.8)$$

Now, the algorithm for solving (IP4) can be summarized as follows. First, from (4.2) we compute  $\omega_{h,H}$ ,  $\{h_n\}_{n=0}^{N_2}$ . Next, with the aid of these coefficients the values  $\dot{\Delta}(\rho_k)$  are computed approximately from (5.8),

$$\dot{\Delta}(\rho_k) \cong \dot{\Delta}_{N_2}(\rho_k) = -(1 + b\omega_{h,H}) \sin(\rho_k b) - \rho_k b \cos(\rho_k b) + \sum_{n=0}^{N_2} h_n \left( b \mathbf{j}_{2n+1}(\rho_k b) - \frac{2n}{\rho_k} \mathbf{j}_{2n}(\rho_k b) \right).$$

Now, the multiplier constants  $\beta_k$  are computed from (5.7). Thus, problem (IP4) is reduced to problem (IP3), and one can apply the algorithm described in the previous section.

## 6 Numerical results

The proposed approach can be implemented directly using an available numerical computing environment. All the reported computations were performed in Matlab R2024a on an Intel i7-1360P equipped laptop computer and took no more than several seconds.

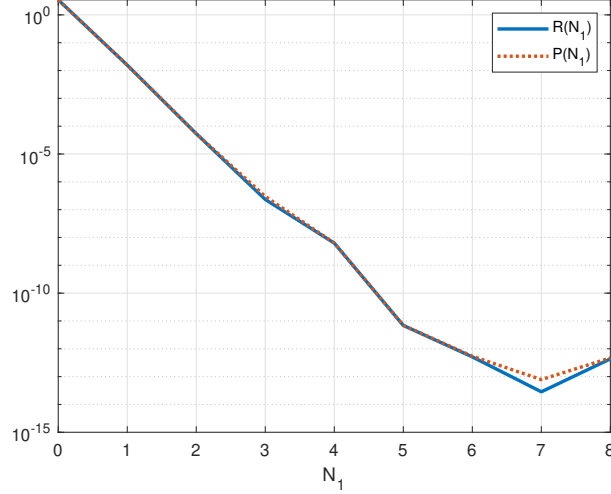


Figure 1:  $P(N_1)$  and  $R(N_1)$  computed for Example 1, with 10 eigenpairs given. Both indicate the choice of  $N_1 = 7$ .

## 6.1 Solution of two-spectrum inverse problem (IP1)

**Example 1.** Consider equation (2.1) with

$$q(x) = x^2, \quad 0 < x < 1, \quad (6.1)$$

and the boundary conditions (2.2) with  $h = 10$  and  $H = \pi$ . For the first test we recover this Sturm-Liouville problem from ten eigenpairs:  $\{\lambda_k, \lambda_k^0\}_{k=0}^9$ . The “exact” eigenvalues were computed by Matslise [36]. The minima of both functionals  $P(N_1)$  and  $R(N_1)$  (see subsection 4.1.3) were attained at  $N_1 = 7$ , see Fig. 1. Thus, in the first step both systems (4.1) and (4.2) were considered with  $K = 9$  and  $N_1 = N_2 = 7$ . It is worth noticing that the parameter  $\omega_{h,H} \cong 13.3082593201899$  was computed from system (4.2) with an absolute error  $3.6 \cdot 10^{-6}$ . For the second step, with the aid of the computed values  $\omega_{h,H}$ ,  $\{\psi_n(0), h_n\}_{n=0}^7$ , the approximate characteristic functions  $\Delta_7^0(\rho)$  and  $\Delta_7(\rho)$  were computed at  $J = 1501$  points  $\rho = r_j$  chosen as follows  $r_j = 10^{\alpha_j}$  with  $\alpha_j$ ,  $j = 1, \dots, J$ , being distributed uniformly on  $[\log(0.01), \log(1000)] = [-2, 3]$ . This is a logarithmically spaced point distribution on the segment  $[0.01, 1000]$ , with points more densely distributed near  $\rho = 0.01$  and less densely distributed as  $\rho$  increases. The parameter  $N_3$  here and in the other numerical tests was chosen equal to  $N_1$ . Thus, system (4.6) consisted of 1501 equations for 24 unknowns. The result of the reconstruction of  $q(x)$  is shown in Fig. 2.

The potential (6.1) on the interval  $(0, 1)$  is a relatively simple example and can be recovered from less eigenpairs. For example, the maximum absolute error of its recovery from five eigenpairs was  $6.8 \cdot 10^{-3}$ . The constants  $h$  and  $H$  were recovered with the absolute error  $4.7 \cdot 10^{-6}$  and  $8.1 \cdot 10^{-6}$ , respectively.

Moreover, the reconstruction procedure results to be stable with respect to a certain level of noise in the input data. The noise is introduced as follows

$$\lambda_{k,\text{noisy}} = \lambda_k + \sigma \sin\left(\frac{(k+1)\pi}{37}\right), \quad k = 0, \dots, K \quad (6.2)$$

and similarly for  $\lambda_k^0$ . Here the coefficient  $\sigma$  determines the level of noise. In the considered example of the reconstruction from five eigenpairs ( $K = 4$ ), we introduced the noise with  $\sigma = 0.001$ . As a result,

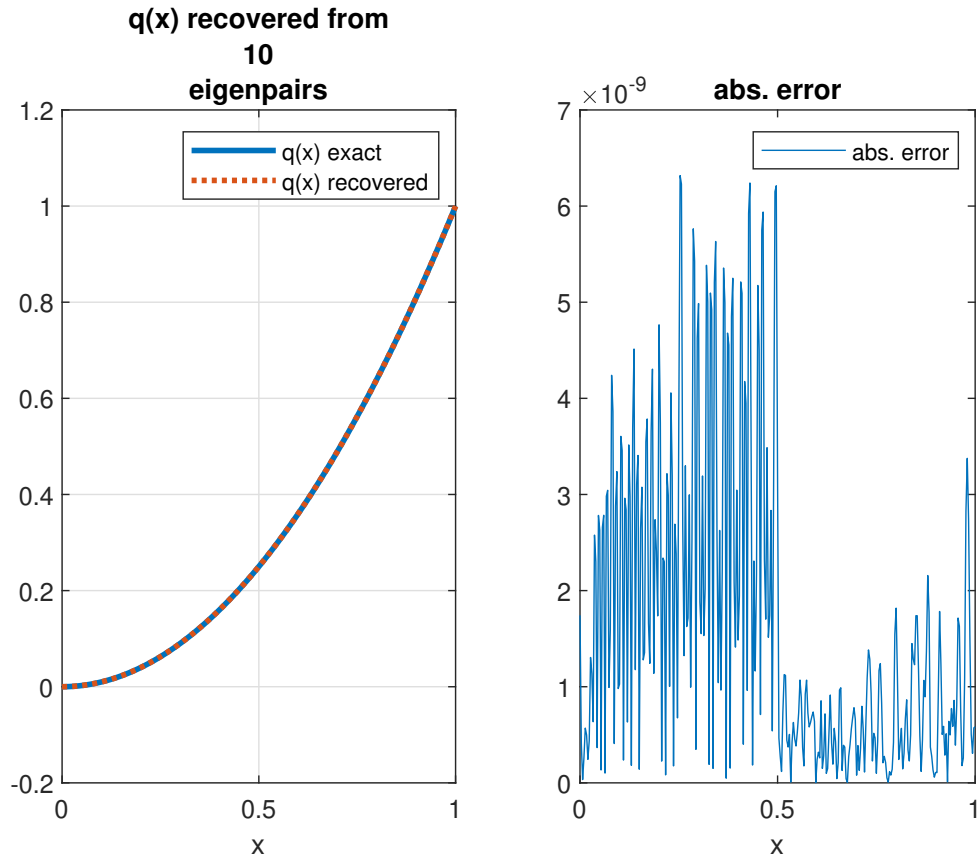


Figure 2: Potential from Example 1, recovered from 10 eigenpairs. The maximum absolute error of the recovered potential is  $6.3 \cdot 10^{-9}$ . The constants  $h = 10$  and  $H = \pi$  are recovered with the absolute error  $3.4 \cdot 10^{-13}$  and  $2.9 \cdot 10^{-12}$ , respectively.

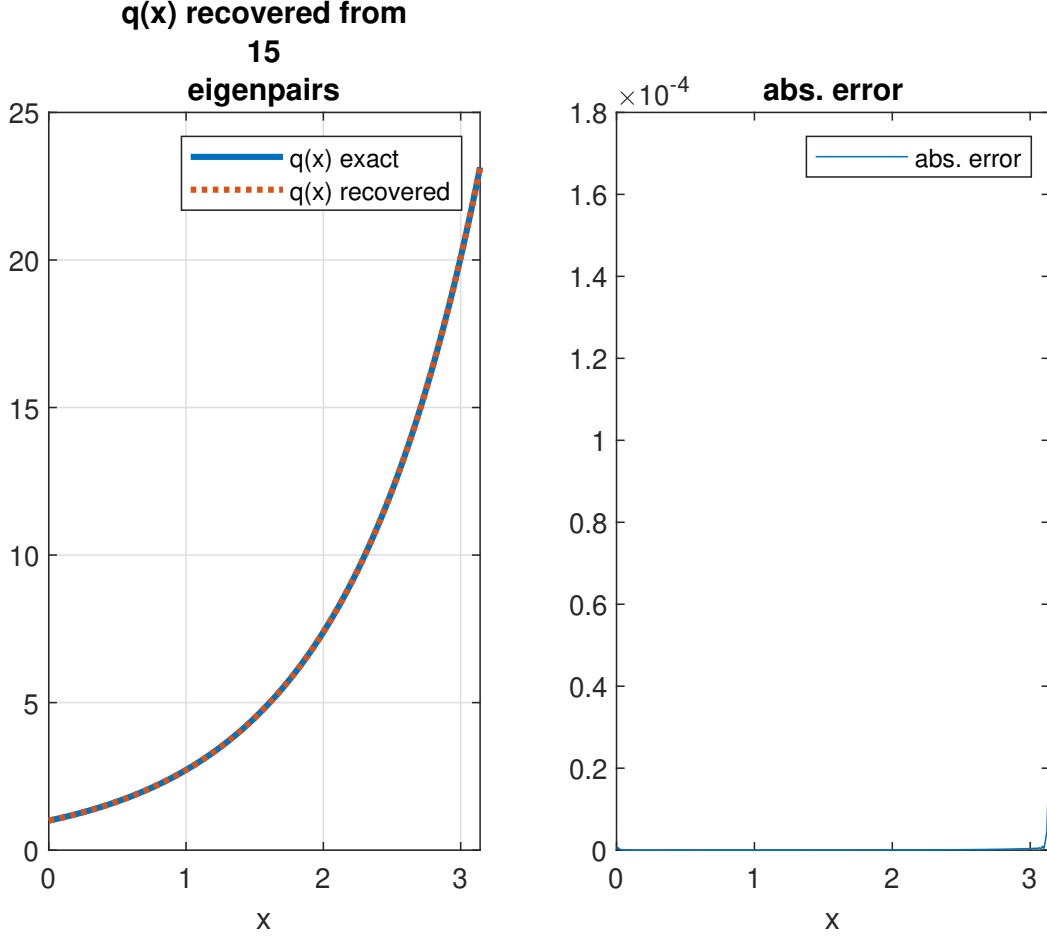


Figure 3: First Paine potential (Example 2) recovered from 15 eigenpairs. The maximum absolute error is  $1.7 \cdot 10^{-4}$ . The constants  $h$  and  $H$  are recovered with the absolute error  $1.6 \cdot 10^{-8}$  and  $6.2 \cdot 10^{-7}$ , respectively.

the potential (6.1) was still recovered quite accurately, with the maximum absolute error of 0.047. The constants  $h$  and  $H$  were recovered with the absolute error  $9.9 \cdot 10^{-5}$  and  $3.1 \cdot 10^{-4}$ , respectively.

In the rest of the numerical tests, for the system of equations (4.6) arising in the last step of the method, we choose the same distribution of the points  $\rho = r_j$ ,  $j = 1, \dots, J$ , as described above in Example 1.

**Example 2.** Consider the potential

$$q(x) = e^x, \quad 0 < x < \pi,$$

and the boundary conditions (2.2) with  $h = 10$  and  $H = \pi$ . Sometimes this potential is called the first Paine potential [42]. The result of its recovery from 15 eigenpairs is shown in Fig. 3. The maximum absolute error resulted in  $1.7 \cdot 10^{-4}$ . The constants  $h$  and  $H$  were recovered with the absolute error  $1.6 \cdot 10^{-8}$  and  $6.2 \cdot 10^{-7}$ , respectively. The parameter  $N_1$  ( $= N_2$ ), as a minimum of  $R(N_1)$ , resulted in its maximum possible value  $N_1 = N_2 = 13$ , which corresponds to the case when system (4.2) is square.

Next, we recovered the same Sturm-Liouville problem from 15 noisy eigenpairs with  $\sigma = 0.01$ .

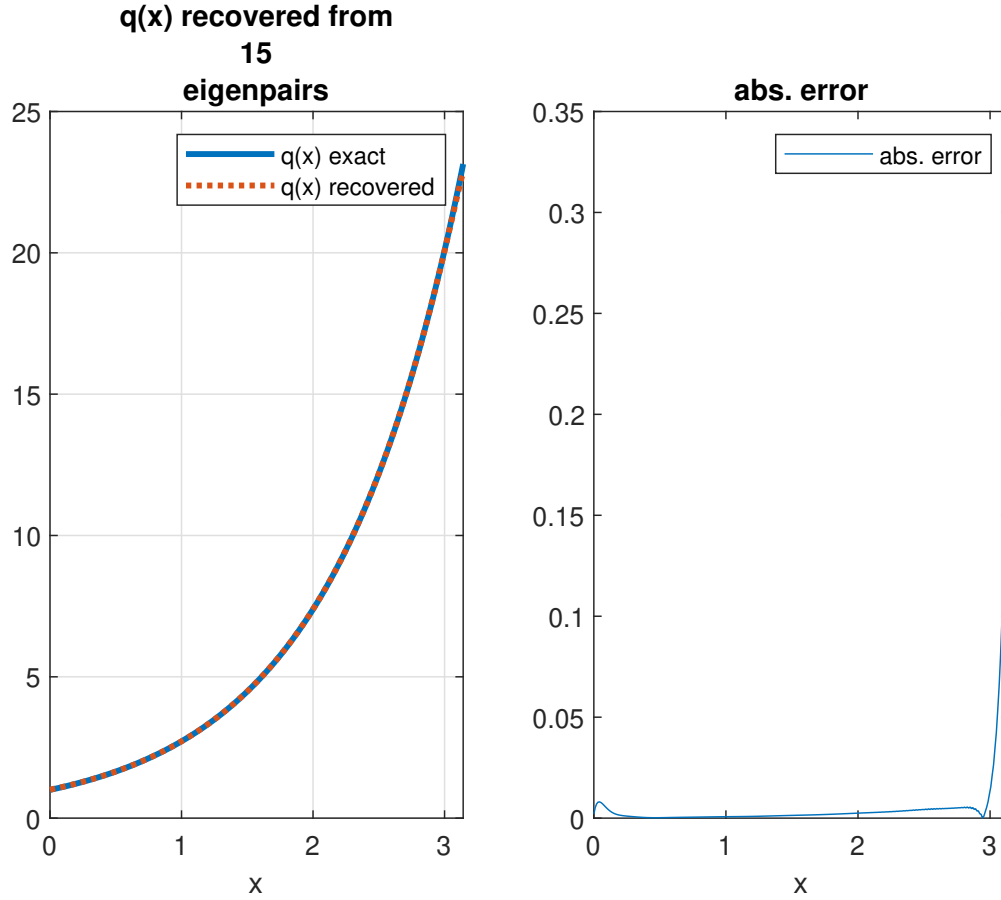


Figure 4: Same as Fig. 3, but recovered from 15 noisy eigenpairs with a high level of noise  $\sigma = 0.01$  (see (6.2)). The maximum absolute error attained at the endpoint  $x = \pi$  resulted in 0.34. The constants  $h$  and  $H$  were recovered with the absolute error  $2.07 \cdot 10^{-4}$  and 0.02, respectively.

This level of noise is high. However, the problem was recovered sufficiently accurately. Fig. 4 shows the result of the recovery of the potential. The maximum absolute error attained at the endpoint  $x = \pi$  resulted in 0.34. The constants  $h$  and  $H$  were recovered with the absolute error  $2.07 \cdot 10^{-4}$  and 0.02, respectively.

The method works equally well for complex-valued potentials. Consider now

$$q(x) = e^x + \pi i, \quad 0 < x < \pi, \quad (6.3)$$

and the same constants  $h$  and  $H$ . Obviously, since the imaginary part of  $q(x)$  is constant, the eigenvalues of the corresponding Sturm-Liouville problems are obtained by adding  $\pi i$  to the eigenvalues of the real valued potential  $\text{Re } q(x)$ . The result of the recovery of  $q(x)$  from 15 noisy eigenpairs with  $\sigma = 0.01$ , is presented in Fig. 5. The maximum absolute error attained at the endpoint  $x = \pi$  resulted in 1.1. The constants  $h$  and  $H$  were recovered with the absolute error 0.0056 and 0.0023, respectively.

**Example 3.** Consider the complex-valued potential

$$q(x) = \left(x^{\frac{\pi}{2}} + \pi\right) \cos(8x) + \pi^2 - i\sqrt{5}, \quad 0 < x < \pi,$$

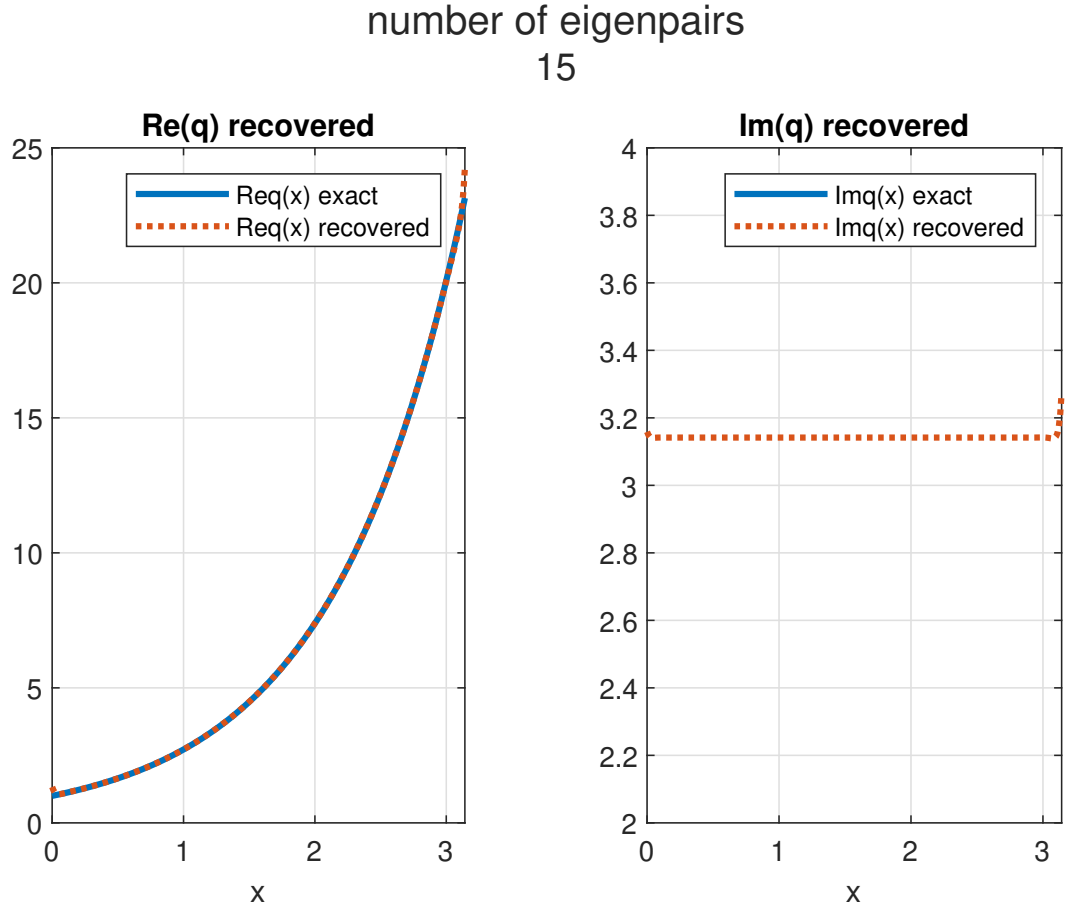


Figure 5: Complex valued otential (6.3) recovered from 15 noisy eigenpairs with  $\sigma = 0.01$ . The maximum absolute error attained at the endpoint  $x = \pi$  resulted in 1.1. The constants  $h$  and  $H$  were recovered with the absolute error 0.0056 and 0.0023, respectively.

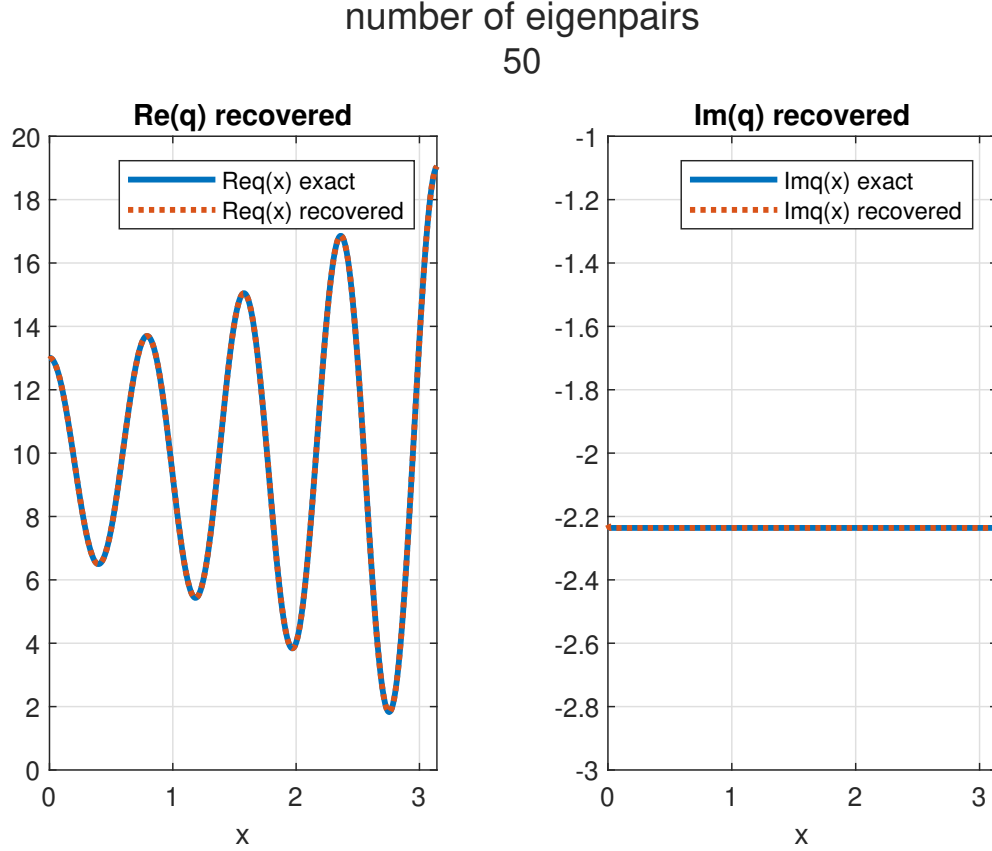


Figure 6: Complex valued potential from Example 3, recovered from 50 eigenpairs. The maximum absolute error of the recovered potential resulted in 0.05, attained at  $x = 0$ . The parameter  $N_1 (= N_2)$ , as a minimum of  $R(N_1)$ , resulted in  $N_1 = 31$ . The constants  $h = \sqrt{2}$  and  $H = -e$  were recovered with the absolute error  $2.8 \cdot 10^{-4}$  and  $1.1 \cdot 10^{-5}$ , respectively.

and the boundary conditions (2.2) with  $h = \sqrt{2}$  and  $H = -e$ . Since the imaginary part of  $q(x)$  is constant, it is not difficult to obtain the eigenpairs by computing them with Matslise for the real part and then adding to them  $\text{Im } q(x)i$ . The recovered potential is shown in Fig. 6. It was computed from 50 eigenpairs. The maximum absolute error of the recovered potential resulted in 0.05, attained at  $x = 0$ . The parameter  $N_1 (= N_2)$ , as a minimum of  $R(N_1)$ , resulted in  $N_1 = 31$ . The constants  $h$  and  $H$  were recovered with the absolute error  $2.8 \cdot 10^{-4}$  and  $1.1 \cdot 10^{-5}$ , respectively.

Next, we reconstructed the same Sturm-Liouville problem from 50 noisy eigenpairs with  $\sigma = 0.001$ . Fig. 7 shows the result. The maximum absolute error of the recovered potential resulted in 0.7, attained at  $x = \pi$ . Again, as in the previous example, the noise in the input data resulted in a smaller value of the parameter  $N_1$ , computed as a minimum of  $R(N_1)$ . We obtained  $N_1 = N_2 = 22$ . The constants  $h$  and  $H$  were recovered with the absolute error  $6 \cdot 10^{-4}$  and  $1.8 \cdot 10^{-3}$ , respectively.

The computation of the eigenvalues for non-selfadjoint Sturm-Liouville problems is, in general, a distinct and challenging task. In the previous two numerical tests, the eigenvalues were computed for selfadjoint problems and subsequently converted to those of the non-selfadjoint problems, as the imaginary part of the potential was simply a constant. The next example is different. It is purely

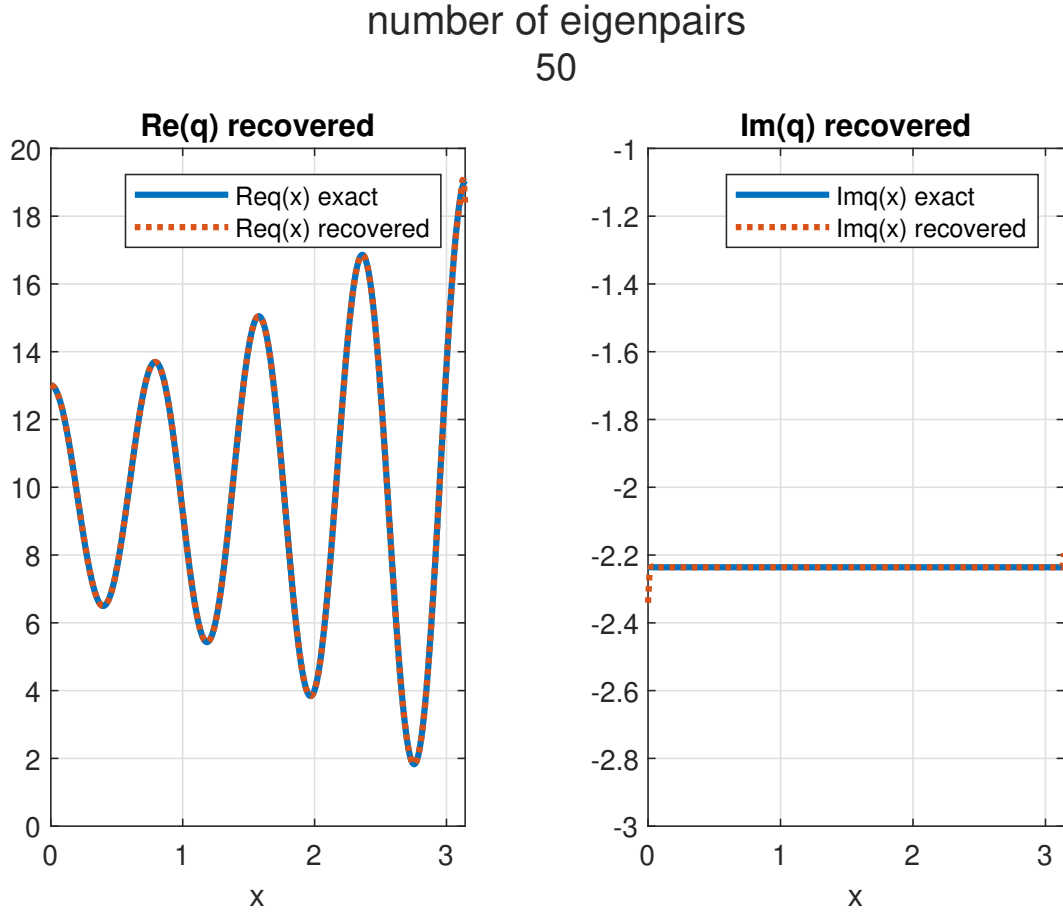


Figure 7: Complex valued potential from Example 3, recovered from 50 noisy eigenpairs with  $\sigma = 0.001$ . The maximum absolute error of the recovered potential resulted in 0.7, attained at  $x = \pi$ . Again, as in the previous example, the noise in the input data resulted in a smaller value of the parameter  $N_1$ , computed as a minimum of  $R(N_1)$ . We obtained  $N_1 = N_2 = 22$ . The constants  $h$  and  $H$  were recovered with the absolute error  $6 \cdot 10^{-4}$  and  $1.8 \cdot 10^{-3}$ , respectively.

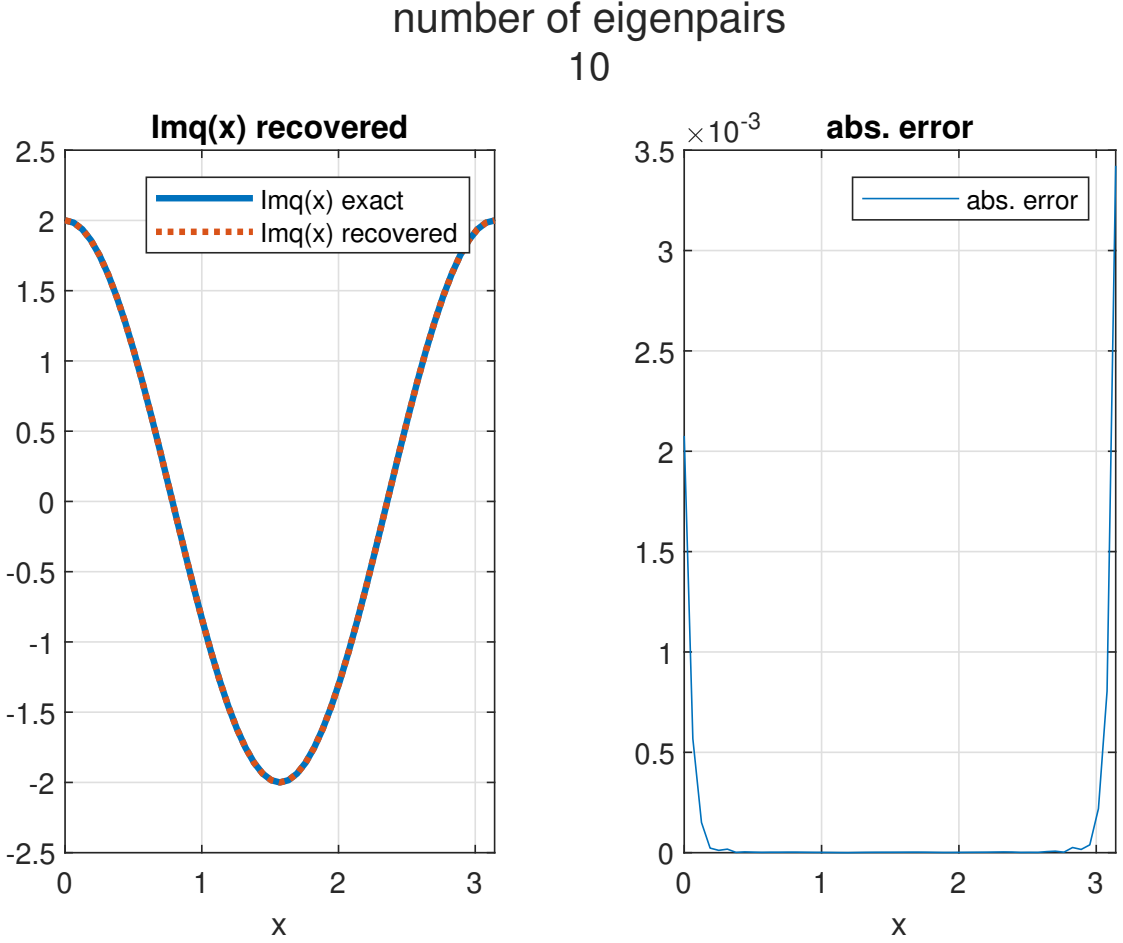


Figure 8: Mathieu potential from Example 4, recovered from ten eigenpairs. The maximum absolute error resulted in  $3.4 \cdot 10^{-3}$ . The constants  $h = 0.7$  and  $H = i$  were recovered with the absolute error  $8.5 \cdot 10^{-5}$  and  $1.2 \cdot 10^{-4}$ , respectively.

imaginary, and the eigenvalues were computed in the framework of [30] with the aid of the NSBF representations and argument principle.

**Example 4.** Consider the Mathieu potential

$$q(x) = is \cos(2x), \quad 0 < x < \pi, \quad (6.4)$$

and the boundary conditions (2.2) with  $h = 0.7$  and  $H = i$ . Let  $s = 2$ . Thus, this inverse problem involves a complex-valued potential and a complex constant in the boundary condition. Fig. 8 shows the result of the recovery of the potential (6.4) from ten eigenpairs. The maximum absolute error resulted in  $3.4 \cdot 10^{-3}$ . The constants  $h$  and  $H$  were recovered with the absolute error  $8.5 \cdot 10^{-5}$  and  $1.2 \cdot 10^{-4}$ , respectively. Thus, these results are more accurate than those reported in [30].

Moreover, the method shows a remarkable stability. Fig. 9 presents the result of the reconstruction of the potential from ten noisy eigenpairs with  $\sigma = 0.001$ . The maximum absolute error resulted in 0.043. The constants  $h$  and  $H$  were recovered with the absolute error  $6 \cdot 10^{-5}$  and  $3 \cdot 10^{-3}$ , respectively.

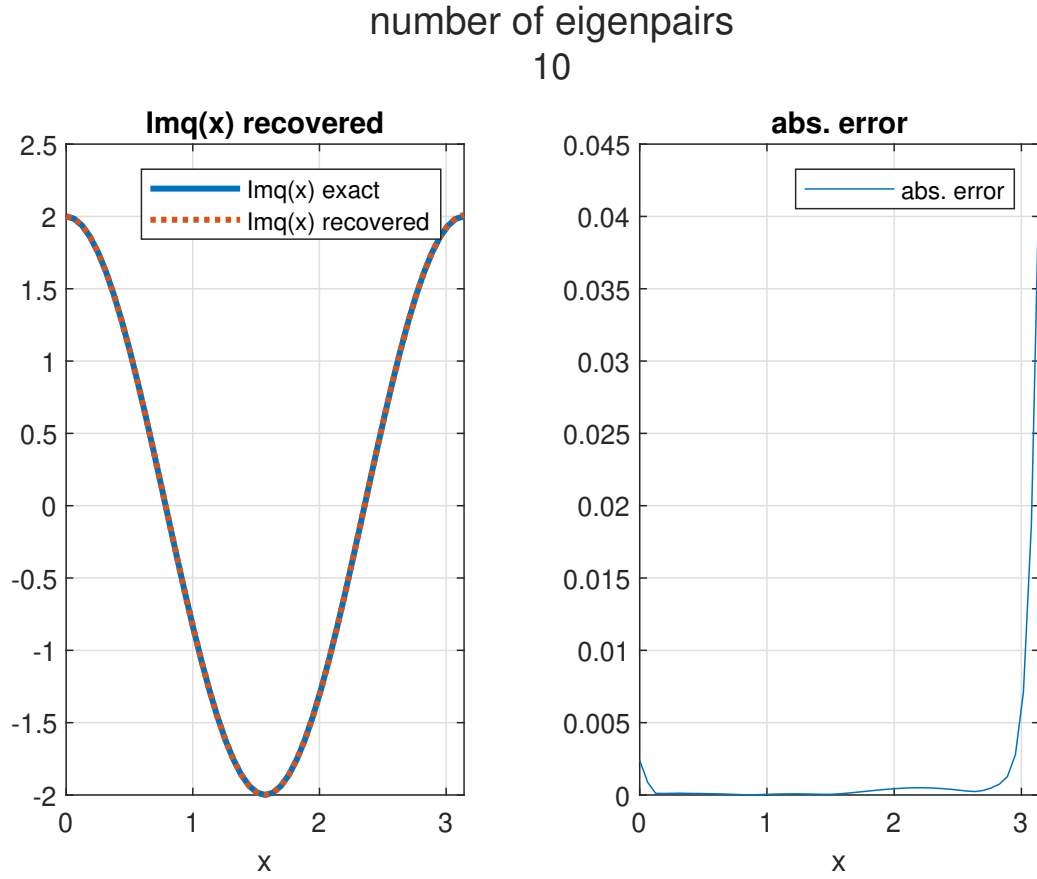


Figure 9: Mathieu potential from Example 4, recovered from ten noisy eigenpairs with  $\sigma = 0.001$ . The maximum absolute error resulted in 0.043. The constants  $h = 0.7$  and  $H = i$  were recovered with the absolute error  $6 \cdot 10^{-5}$  and  $3 \cdot 10^{-3}$ , respectively.

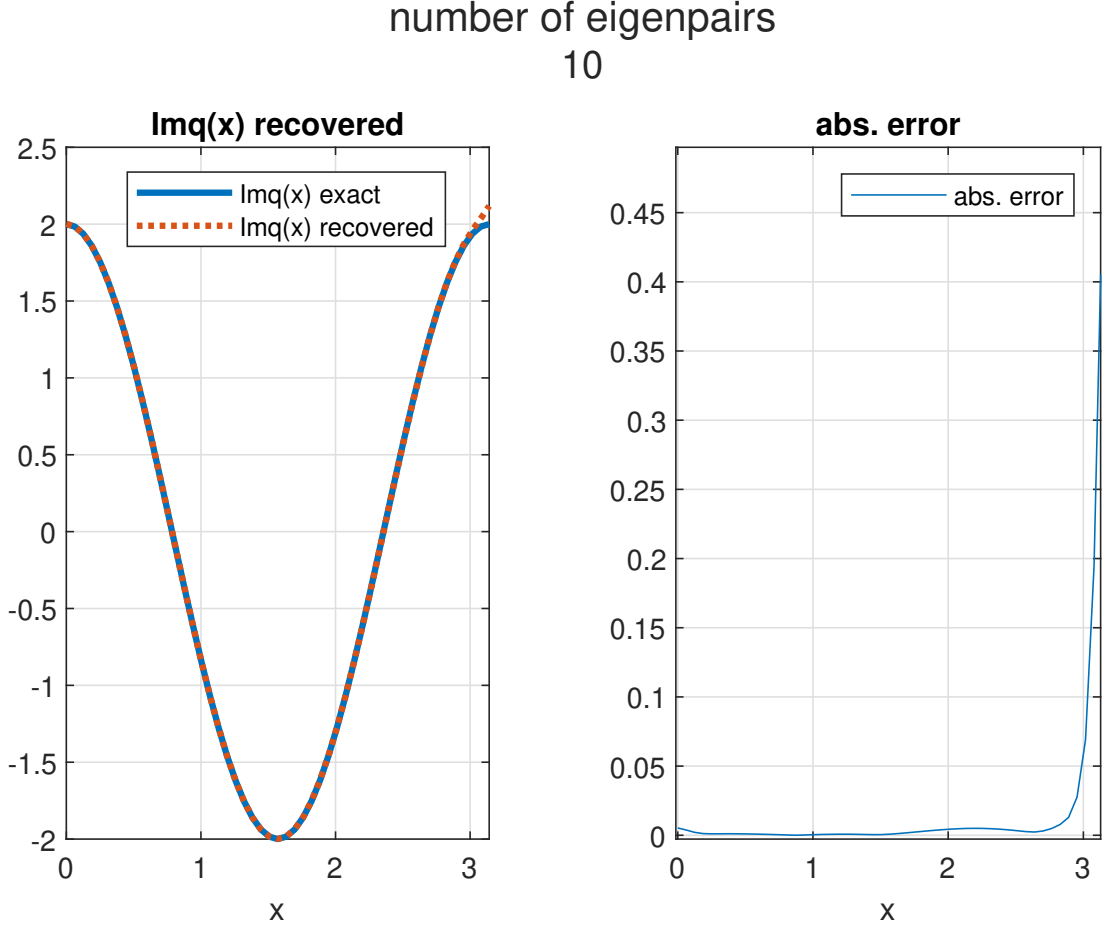


Figure 10: Mathieu potential from Example 4, recovered from ten noisy eigenpairs with  $\sigma = 0.01$ . The maximum absolute error resulted in 0.46. The constants  $h$  and  $H$  were recovered with the absolute error  $3.12 \cdot 10^{-4}$  and 0.032, respectively.

A greater level of noise:  $\sigma = 0.01$  still allows to recover the Sturm-Liouville problem quite accurately, see Fig. 10. The maximum absolute error resulted in 0.46. The constants  $h$  and  $H$  were recovered with the absolute error  $3.12 \cdot 10^{-4}$  and 0.032, respectively.

Even the level of noise  $\sigma = 0.1$  still allows one to obtain a meaningful approximation, see Fig.11. The constants  $h$  and  $H$  were recovered with the absolute error 0.0036 and 0.32, respectively.

## 6.2 Reconstruction from Weyl function, problem (IP2)

The Weyl functions of the Sturm-Liouville problems considered in this subsection were computed by the formula

$$M(\rho) = -\frac{\Delta^0(\rho)}{\Delta(\rho)},$$

where in their turn,  $\Delta^0(\rho)$  and  $\Delta(\rho)$  were computed with the aid of the NSBF representations (3.4), (3.5), (3.11), (3.12), with the coefficients calculated following the recurrent integration procedure from

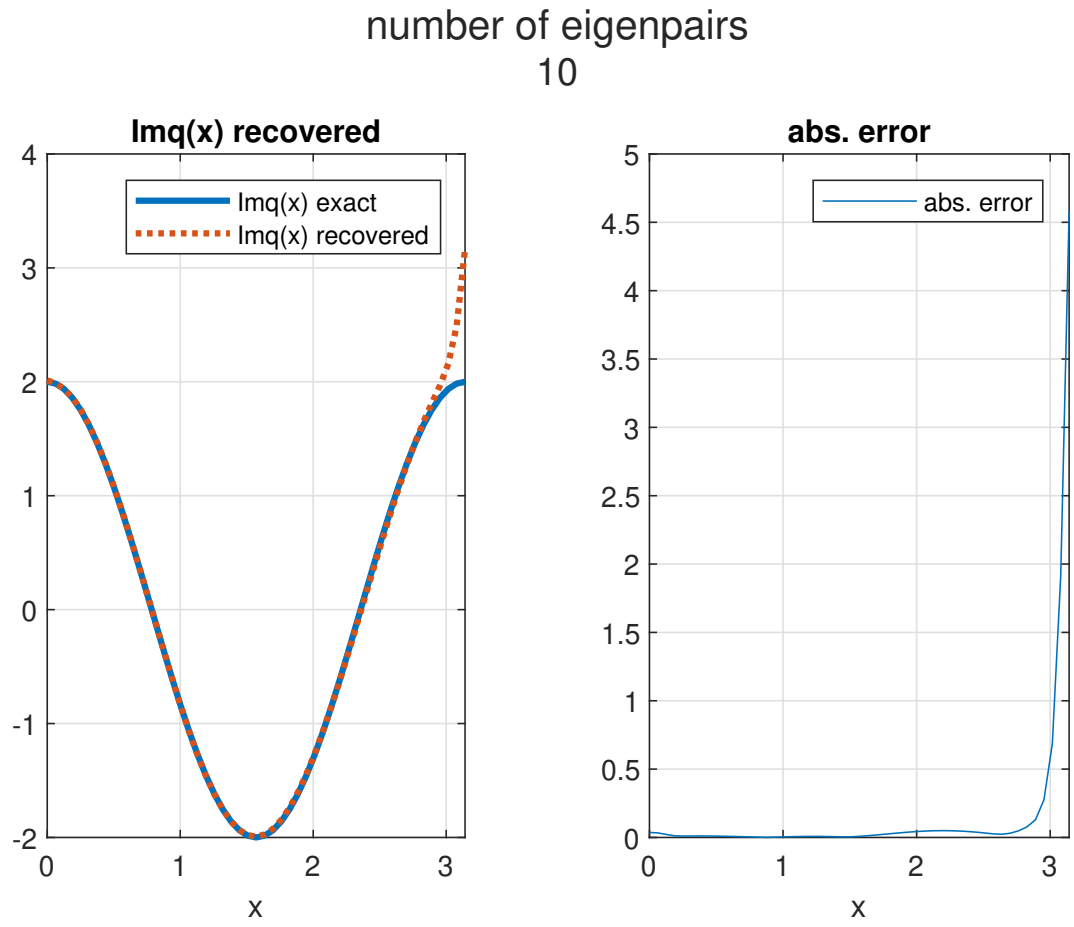


Figure 11: Mathieu potential from Example 4, recovered from ten noisy eigenpairs with  $\sigma = 0.1$ . The constants  $h$  and  $H$  were recovered with the absolute error 0.0036 and 0.32, respectively.

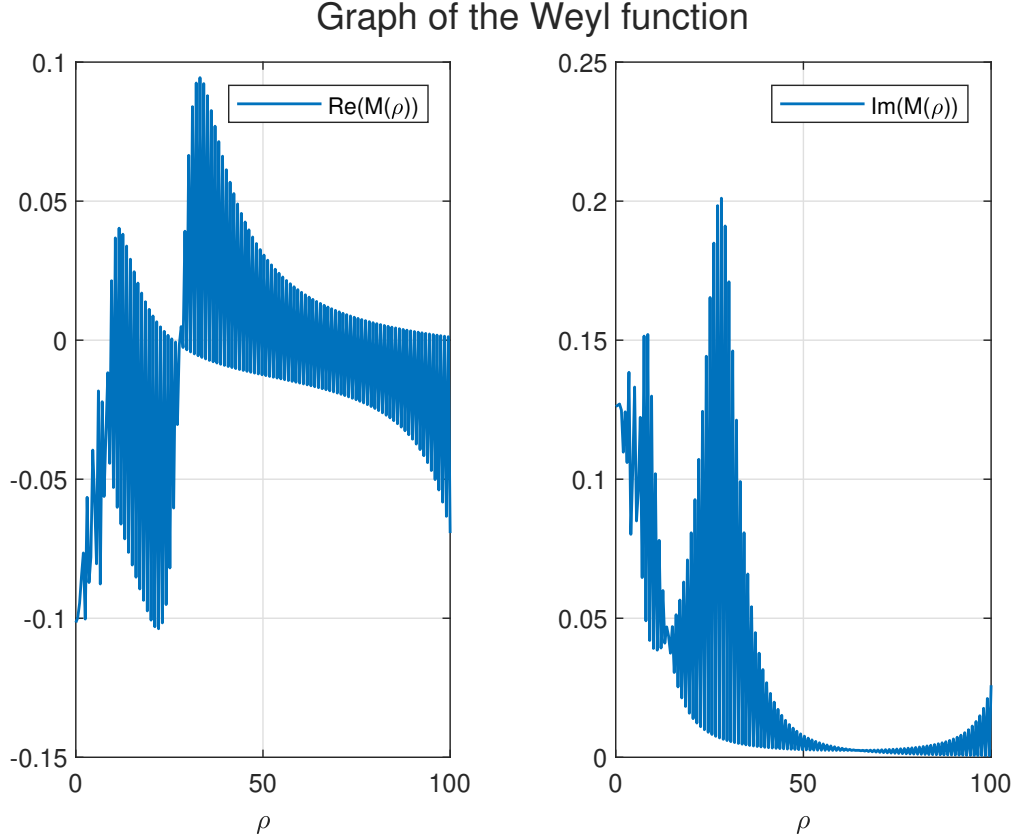


Figure 12: Weyl function of Sturm-Liouville problem from Example 5 on the segment  $[0.01, 100]$ .

[31] (see also [26]).

**Example 5.** Consider problem  $L$  with the complex-valued potential and complex constants in the boundary conditions:

$$q(x) = e^x + \frac{i}{(x + 0.1)^2}, \quad x \in [0, \pi],$$

$$h = 1 - i, \quad H = e^i.$$

Thus, the real and imaginary parts of the potential are the two Paine potentials (see, e.g., [42], [43]).

As the data for the inverse problem, the values of  $M(\rho)$  were given at 2000 points logarithmically spaced along the segment  $[0.01, 1000]$ , and additionally at 20 points  $\rho_j$  distributed uniformly on the segment  $[0.01, 1000]$ . These last 20 points were used for choosing an appropriate value of the parameter  $N_1$  in (5.2). Namely,  $N_1$  was chosen by minimizing the functional  $Q(N_1) = \max_{\rho_j} |\Delta_{N_1}^0(\rho) + M(\rho)\Delta_{N_1}(\rho)|$ .

The Weyl function computed on the segment  $[0.01, 100]$  is depicted in Fig. 12.

Fig. 13 presents the result of the reconstruction of the potential  $q(x)$ . The maximum absolute error was 1.57 attained at the origin (the relative error was approximately 0.0157). The constants  $h$  and  $H$  were recovered with the absolute error 0.0044 and 0.0013, respectively. The parameter  $N_1$  in (5.2) resulted in 33.

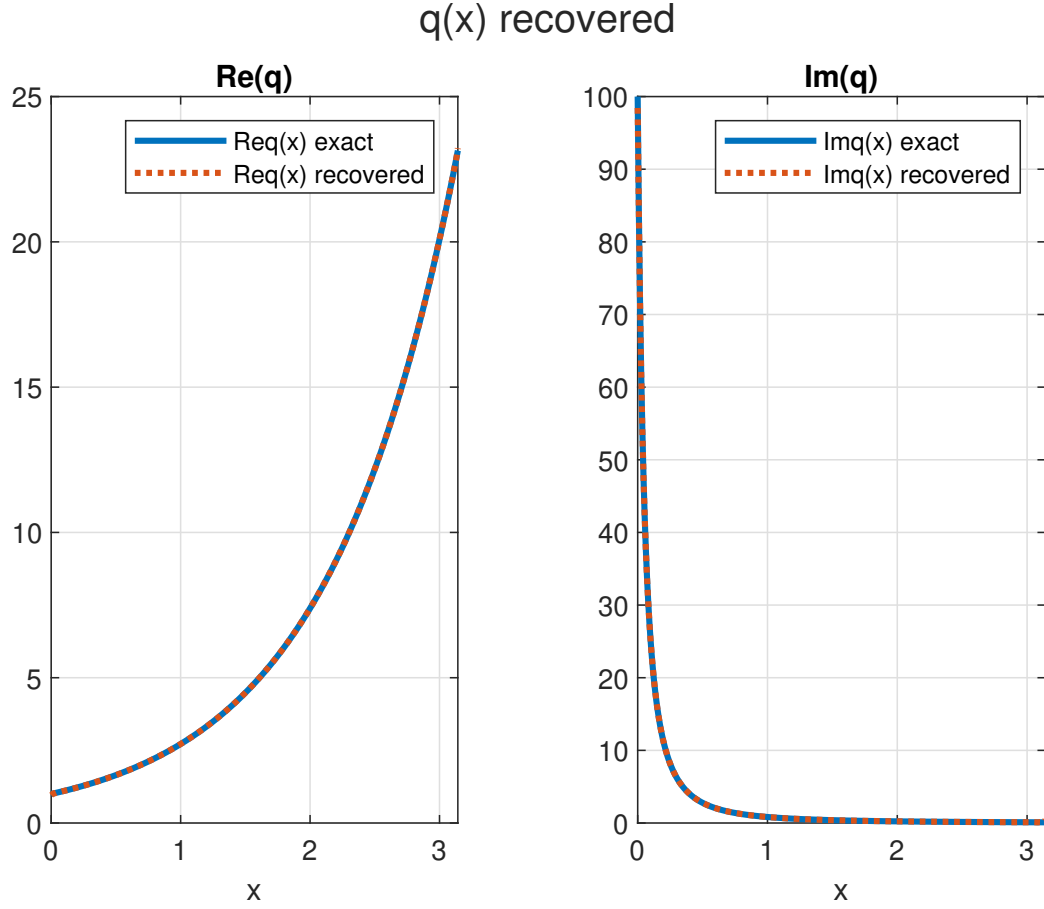


Figure 13: Potential from Example 5 recovered from  $M(\rho)$  given at 2000 points logarithmically spaced along the segment  $[0.01, 1000]$ . The maximum absolute error was 1.57 attained at the origin (the relative error was approximately 0.0157). The constants  $h$  and  $H$  were recovered with the absolute error 0.0044 and 0.0013, respectively. The parameter  $N_1$  in (5.2) resulted in 33.

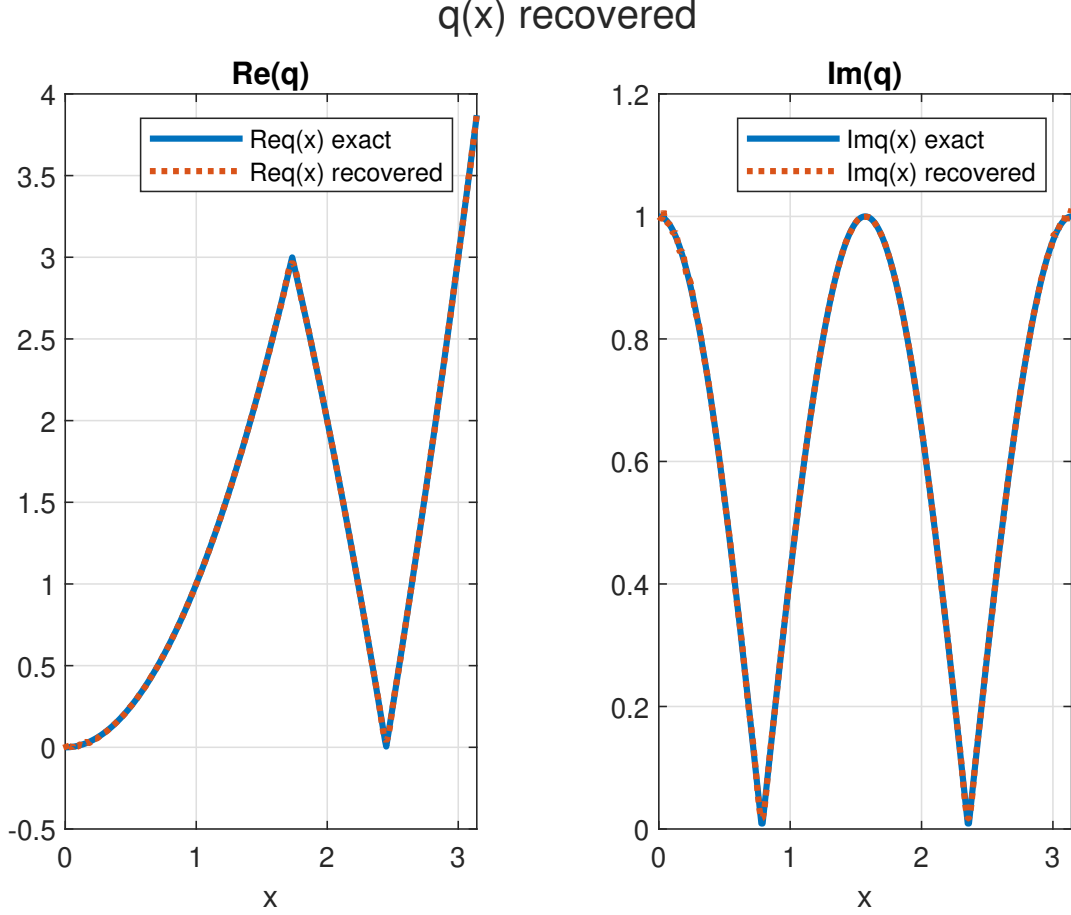


Figure 14: Potential from Example 6 recovered from the Weyl function  $M(\rho)$  given at 2000 points logarithmically spaced on the segment  $[0.01, 1000]$ . The maximum absolute error resulted in 0.036. The constants  $h$  and  $H$  were recovered with the absolute error  $7.4 \cdot 10^{-6}$  and  $1.4 \cdot 10^{-4}$ , respectively.

**Example 6.** Consider problem  $L$  with a less smooth potential

$$q(x) = |3 - |x^2 - 3|| + i |\cos(2x)|, \quad x \in [0, \pi],$$

$$h = e^{2i}, \quad H = \pi - i.$$

The Weyl function  $M(\rho)$  was given at 2000 points logarithmically spaced on the segment  $[0.01, 1000]$ .

Fig. 14 presents the result of the reconstruction of the potential  $q(x)$ . The maximum absolute error resulted in 0.036. The constants  $h$  and  $H$  were recovered with the absolute error  $7.4 \cdot 10^{-6}$  and  $1.4 \cdot 10^{-4}$ , respectively. The parameter  $N_1$  in (5.2) resulted in 49. This value was obtained by minimizing the value of the functional  $Q(N_1) = |\Delta_{N_1}^0(\rho) + M(\rho)\Delta_{N_1}(\rho)|$  evaluated at 20 points  $\rho_j$  distributed uniformly on the segment  $[0.01, 1000]$ .

### 6.3 Reconstruction from eigenvalues and multiplier constants, problem (IP3)

The multiplier constants  $\beta_k$  required as a part of the input data of problem (IP3) are computed from (5.4), where  $\varphi_h(\rho_k, b)$  are computed by calculating the NSBF representations with the aid of the

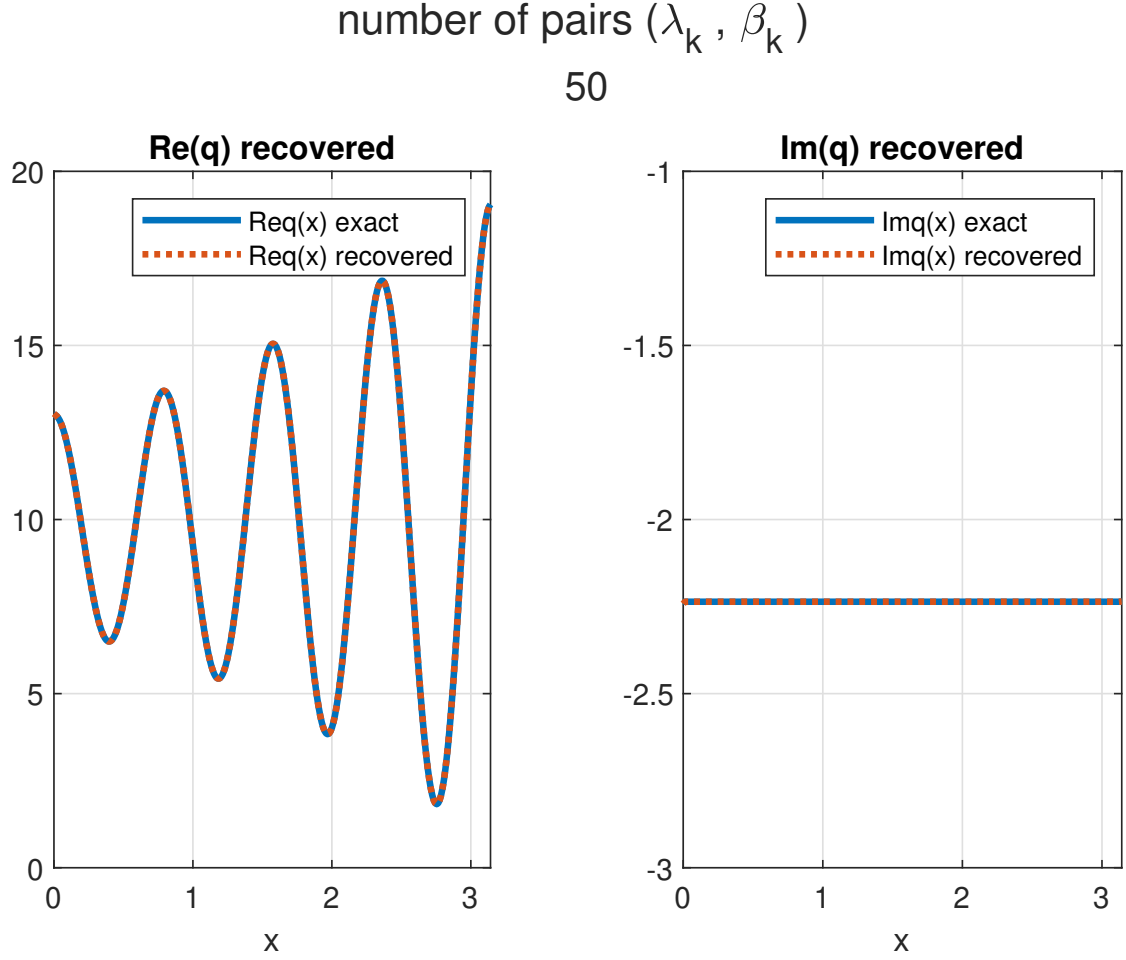


Figure 15: Complex valued potential from Example 3 recovered from 50 pairs  $(\lambda_k, \beta_k)$ . The constants  $h = \sqrt{2}$  and  $H = -e$  were recovered with the absolute error  $8.5 \cdot 10^{-5}$  and  $6.21 \cdot 10^{-5}$ , respectively.

recurrent integration procedure, as explained in [31].

**Example 7.** Consider the inverse problem (IP3) for the complex-valued potential  $q(x)$  and constants  $h$  and  $H$  from Example 3. Fig. 15 presents the result of the recovery of  $q(x)$  from 50 pairs  $(\lambda_k, \beta_k)$ . The maximum absolute error resulted in 0.03. The constants  $h$  and  $H$  were recovered with the absolute error  $8.5 \cdot 10^{-5}$  and  $6.21 \cdot 10^{-5}$ , respectively.

**Example 8.** Consider the inverse problem (IP3) for the complex-valued potential  $q(x)$  and constants  $h$  and  $H$  from Example 4. Fig. 16 presents the result of the recovery of  $q(x)$  from 10 pairs  $(\lambda_k, \beta_k)$ . The maximum absolute error resulted in 0.0034. The constants  $h$  and  $H$  were recovered with the absolute error  $1.56 \cdot 10^{-4}$  and  $1.2 \cdot 10^{-4}$ , respectively. The result is similar to that for problem (IP1), compare to Fig. 8.

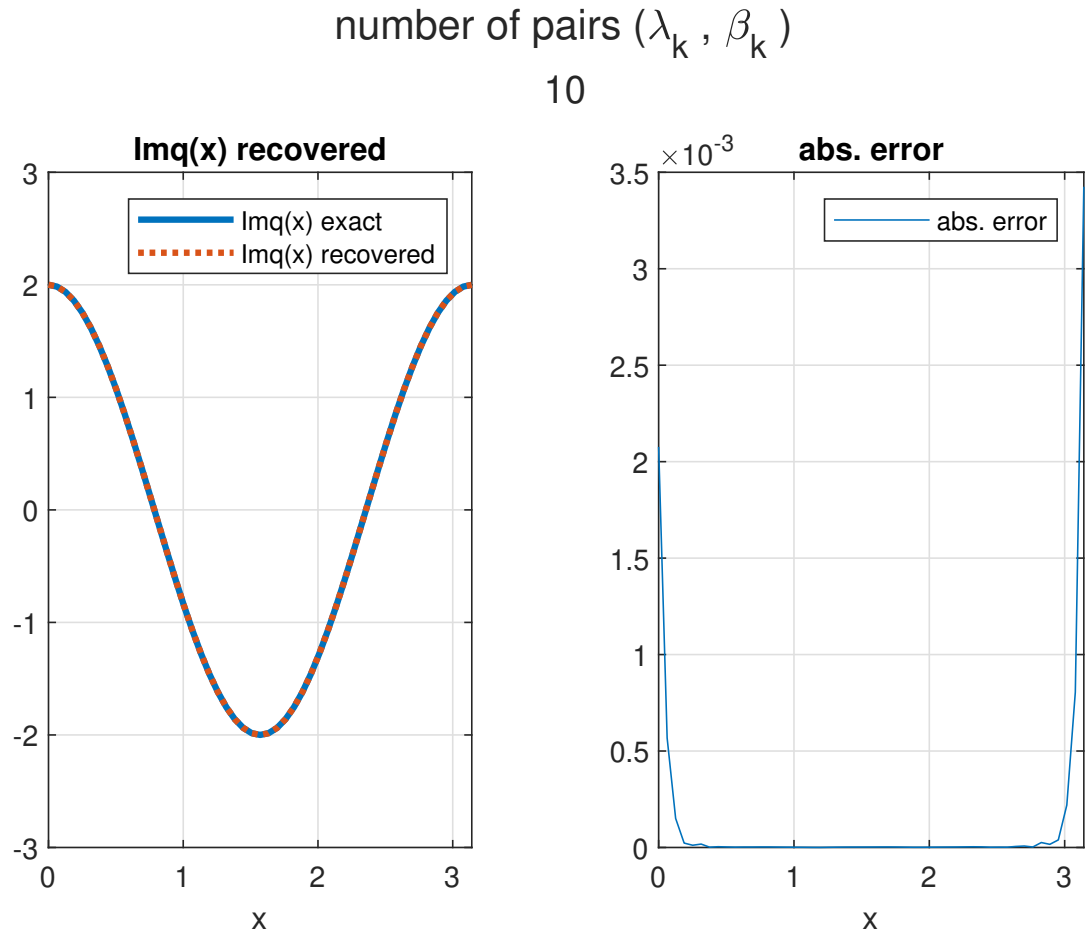


Figure 16: Complex valued Mathieu potential from Example 4 recovered from 10 pairs  $(\lambda_k, \beta_k)$ . The maximum absolute error resulted in 0.0034. The constants  $h$  and  $H$  were recovered with the absolute error  $1.56 \cdot 10^{-4}$  and  $1.2 \cdot 10^{-4}$ , respectively.

## 6.4 Reconstruction from eigenvalues and norming constants, problem (IP4)

Since problem (IP4) reduces to problem (IP3) by computing first  $\dot{\Delta}(\rho_k)$  and next the multiplier constants  $\beta_k$ , as explained in subsection 5.3, here the main question is how accurate is this reduction procedure. Let us consider an example. For the Sturm-Liouville problem from Example 2 we computed the norming constants with the aid of Matslise. This was done as follows. Matslise allows one to compute normalized eigenfunctions of selfadjoint Sturm-Liouville problems  $u_k(x)$ :  $\|u_k\|_{\mathcal{L}^2(0,b)} = 1$ . Clearly,  $\varphi_h(\rho_k, x) = u_k(x)/u_k(0)$ , and hence

$$\alpha_k = \int_0^b \varphi_h^2(\rho_k, x) dx = \frac{1}{u_k^2(0)} \int_0^b u_k^2(x) dx = \frac{1}{u_k^2(0)}.$$

The values  $u_k(0)$  were computed by Matslise.

We computed first fifteen norming constants for the Sturm-Liouville problem from Example 2, and then with their aid, the values  $\dot{\Delta}(\rho_k)$  and the multiplier constants  $\beta_k$ . We compared them to those computed as explained in subsection 6.3. The maximum resulting difference was  $2.8 \cdot 10^{-10}$ . Thus, indeed, the proposed procedure provides an accurate reduction of problem (IP4) to problem (IP3).

## 7 Conclusions

In this work a method for solving a variety of inverse spectral problems for Sturm-Liouville equations with complex coefficients is presented. It is based on the Neumann series of Bessel functions representations for solutions of the Sturm-Liouville equations. The series representations possess several remarkable features which make them especially convenient for solving inverse problems. Most important, with respect to the spectral parameter  $\rho = \sqrt{\lambda}$  the series converge uniformly in any strip parallel to the real axis, and the very first coefficients of the series contain all the information on the Sturm-Liouville problem. Thus, the solution of the inverse problems reduces to the solution of one or two systems of linear algebraic coefficients for the coefficients of the series. The method is easy for implementation, direct, accurate and applicable to a large variety of inverse problems. Its performance is illustrated by numerical examples.

**Acknowledgments** The author thanks Lady Estefania Murcia Lozano for providing the eigenvalues for Example 4.

**Funding information** CONAHCYT, Mexico, grant ‘‘Ciencia de Frontera’’ FORDECYT - PRONACES/61517/ 2020.

**Data availability** The data that support the findings of this study are available upon reasonable request.

**Conflict of interest** This work does not have any conflict of interest.

## References

- [1] M. Abramovitz and I. A. Stegun, Handbook of mathematical functions (Dover, New York, 1972).
- [2] L. E. Andersson, Algorithms for solving inverse eigenvalue problems for Sturm-Liouville equations, in: Sabatier, P.C. (ed.) Inverse Methods in Action, 138-145 (Springer-Verlag, Berlin, 1990).
- [3] S. A. Avdonin, K. V. Khmelnytskaya, V. V. Kravchenko, Recovery of a potential on a quantum star graph from Weyl’s matrix. Inverse Problems and Imaging, 18(1) (2024), 311-325.
- [4] S. A. Avdonin, K. V. Khmelnytskaya, V. V. Kravchenko Reconstruction techniques for quantum trees. Mathematical Methods in the Applied Sciences, 47 (2024), 7182-7197.

- [5] S. A. Avdonin, V. V. Kravchenko, Method for solving inverse spectral problems on quantum star graphs. *Journal of Inverse and Ill-posed Problems*, 31 (2023), 31-42.
- [6] C. Böckmann, A. Kammanee, Broyden method for inverse non-symmetric Sturm-Liouville problems, *Bit Numer Math* 51 (2011), 513–528.
- [7] L. Borcea, V. Druskin, and L. Knizhnerman On the continuum limit of a discrete inverse spectral problem on optimal finite difference grids. *Comm. Pure Appl. Math.* 58 (9) (2005), 1231 - 1279.
- [8] B.M. Brown, R.A. Peacock, R.Weikard, A local Borg–Marchenko theorem for complex potentials. *Journal of Computational and Applied Mathematics* 148 (2002), 115–131.
- [9] B. M. Brown, V. S. Samko, I. W. Knowles, M. Marletta, Inverse spectral problem for the Sturm–Liouville equation, *Inverse Probl.* 19 (2003), 235–252.
- [10] S.A. Buterin, On inverse spectral problem for non-selfadjoint Sturm–Liouville operator on a finite interval, *J. Math. Anal. Appl.* 335 (2007) 739–749.
- [11] S. A. Buterin, M. Kuznetsova, On Borg’s method for non-selfadjoint Sturm–Liouville operators. *Anal. Math. Phys.* 9 (2019), 2133–2150.
- [12] F. A. Çetinkaya, K. V. Khmelnytskaya, V. V. Kravchenko, Neumann series of Bessel functions for inverse coefficient problems. *Mathematical Methods in the Applied Sciences*, 47(16) (2024), 12373–12387.
- [13] B. B. Delgado, K. V. Khmelnytskaya, V. V. Kravchenko, The transmutation operator method for efficient solution of the inverse Sturm-Liouville problem on a half-line. *Mathematical Methods in the Applied Sciences*, 42(18) (2019), 7359-7366.
- [14] M.-C. Drignei, A Newton-type method for solving an inverse Sturm-Liouville problem, *Inverse Probl. Sci. Eng.* 23 (2015) 851–883.
- [15] G. Freiling, V. Yurko, *Inverse Sturm-Liouville problems and their applications*. Nova Science Publishers Inc., Huntington, NY, 2001.
- [16] Q. Gao, Decent flow methods for inverse Sturm–Liouville problem, *Appl. Math. Modelling* 36 (2012), 4452–4465.
- [17] Q. Gao, X. Cheng, Zh. Huang, Modified Numerov’s method for inverse Sturm–Liouville problems, *J. Comput. Appl. Math.* 253 (2013), 181–199.
- [18] Q. Gao, X. Cheng, Zh. Huang, On a boundary value method for computing Sturm–Liouville potentials from two spectra, *Int. J. Comput. Math.* 91 (2014), 490–513.
- [19] Q. Gao, Z. Huang, and X. Cheng, A finite difference method for an inverse Sturm-Liouville problem in impedance form, *Numer. Algor.* 70 (2015), 669-690.
- [20] M. Ignatiev, V. Yurko, Numerical methods for solving inverse Sturm-Liouville problems, *Results Math.* 52, no. 1–2 (2008), 63–74.
- [21] A. Kammanee, C. Böckmann, Boundary value method for inverse Sturm-Liouville problems, *Appl. Math. Comput.* 214 (2009), 342–352.
- [22] A.N. Karapetyants, and V.V. Kravchenko, *Methods of mathematical physics: classical and modern* (Birkhäuser, Cham, 2022).
- [23] A. N. Karapetyants, K. V. Khmelnytskaya, V. V. Kravchenko, A practical method for solving the inverse quantum scattering problem on a half line. *Journal of Physics: Conference Series*, 1540 (2020), 012007.
- [24] K. V. Khmelnytskaya, V. V. Kravchenko, S. M. Torba, A representation of the transmutation kernels for the Schrödinger operator in terms of eigenfunctions and applications. *Applied Mathematics and Computation*, 353 (2019), 274-281.
- [25] V. V. Kravchenko, On a method for solving the inverse Sturm–Liouville problem. *J. Inverse Ill-posed Probl.* 27 (2019), 401-407.

- [26] V. V. Kravchenko, Direct and inverse Sturm-Liouville problems: A method of solution (Birkhäuser, Cham, 2020).
- [27] V. V. Kravchenko, Spectrum completion and inverse Sturm-Liouville problems. *Mathematical Methods in the Applied Sciences*, 46 (2023), 5821-5835.
- [28] V. V. Kravchenko, Reconstruction techniques for complex potentials. *J. Math. Phys.* 65 (3) (2024), 033501.
- [29] V. V. Kravchenko, K. V. Khmelnytskaya, F. A. Çetinkaya, Recovery of inhomogeneity from output boundary data. *Mathematics*, 10 (2022), 4349.
- [30] V. V. Kravchenko, L. E. Murcia-Lozano, Sinc method in spectrum completion and inverse Sturm-Liouville problems. *Mathematical Methods in the Applied Sciences*, 48(3) (2025), 3130–3169.
- [31] V. V. Kravchenko, L. J. Navarro, and S. M. Torba, Representation of solutions to the one-dimensional Schrödinger equation in terms of Neumann series of Bessel functions, *Appl. Math. Comput.* 314 (2017), 173–192.
- [32] V. V. Kravchenko, E. L. Shishkina, S. M. Torba, A transmutation operator method for solving the inverse quantum scattering problem. *Inverse Problems*, 36 (2020), 125007.
- [33] V. V. Kravchenko, S. M. Torba, A direct method for solving inverse Sturm-Liouville problems, *Inverse Problems* 37 (2021), 015015.
- [34] V. V. Kravchenko, S. M. Torba, A practical method for recovering Sturm-Liouville problems from the Weyl function. *Inverse Problems* 37, 065011 (2021).
- [35] V. V. Kravchenko, V. A. Vicente-Benitez, Transmutation operators method for Sturm-Liouville equations in impedance form II: Inverse problem, *Journal of Mathematical Sciences*, 266(4) (2022), 554-575.
- [36] V. Ledoux, M. V. Daele, and G. V. Berghe, MATSLISE: a MATLAB package for the numerical solution of Sturm-Liouville and Schrödinger equations, *ACM Trans. Math. Softw.* 31 (2005), 532–554.
- [37] B. M. Levitan, *Inverse Sturm-Liouville problems*, VSP, Zeist, 1987.
- [38] B. D. Lowe, M. Pilant, W. Rundell, The recovery of potentials from finite spectral data, *SIAM J. Math. Anal.* 23 (1992), 482–504.
- [39] A. Neamaty, Sh. Akbarpoor, E. Yilmaz, Solving inverse Sturm-Liouville problem with separated boundary conditions by using two different input data, *Int. J. Comput. Math.* 95 (2018), 1992–2010.
- [40] A. Neamaty, Sh. Akbarpoor, E. Yilmaz, Solving symmetric inverse Sturm-Liouville problem using Chebyshev polynomials, *Mediterr. J. Math.* (2019) 16:74.
- [41] V. A. Marchenko, *Sturm-Liouville Operators and Applications: Revised Edition*. AMS Chelsea Publishing, Providence, (2011).
- [42] J. W. Paine, F. R. de Hoog, R. S. Anderssen, On the correction of finite difference eigenvalue approximations for Sturm-Liouville problems. *Computing* 26 (1981), 123–139.
- [43] J. D. Pryce, *Numerical solution of Sturm-Liouville problems*, Clarendon Press, Oxford, 1993.
- [44] N. Röhrli, A least squares functional for solving inverse Sturm-Liouville problems, *Inverse Probl.* 21 (2005), 2009–2017.
- [45] W. Rundell, and P. E. Sacks, Reconstruction techniques for classical inverse Sturm-Liouville problems, *Math. Comput.* 58 (1992), 161–183.
- [46] P. E. Sacks, An iterative method for the inverse Dirichlet problem, *Inverse Probl.* 4 (1988), 1055-1069.
- [47] E. L. Shishkina, S. M. Sitnik, *Transmutations, singular and fractional differential equations with applications to mathematical physics*, Elsevier, Amsterdam, 2020.
- [48] G. N. Watson, *A Treatise on the theory of Bessel functions* (Cambridge University Press, Cambridge, 1980).

- [49] J. E. Wilkins, Neumann series of Bessel functions. *Trans. Amer. Math. Soc.* 64 (1948), 359–385.
- [50] V. A. Yurko, Introduction to the theory of inverse spectral problems, Fizmatlit, Moscow, 2007 (in Russian).